



CHALMERS
UNIVERSITY OF TECHNOLOGY

Structural Design of a Wooden Wind Tower Structure

Master's thesis in Applied Mechanics

PETRA STEEN

MASTER'S THESIS 2017:83

Structural Design of a Wooden Wind Tower Structure

PETRA STEEN



Department of Applied Mechanics
CHALMERS UNIVERSITY OF TECHNOLOGY
Gothenburg, Sweden 2017

Structural Design of a Wooden Wind Tower Structure
PETRA STEEN

© PETRA STEEN, 2017.

Examiner: Mats Ander, Department of Applied Mechanics
Supervisors: Joakim Örneblad and Otto Lundman, Modvion AB

Master's Thesis 2017:83
ISSN 1652-8557
Department of Applied Mechanics
Chalmers University of Technology
SE-412 96 Gothenburg
Telephone +46 31 772 1000

Abstract

A modular design of a wooden wind turbine support structure is developed by Modvion. The distinction between the commonly used steel towers are the tall height of 120 m and that it is made out of wood, which enlarges the dimensions of the structure in order to endure the loading. The thesis work primarily covers the initial structural design of the support structure adopting an analytical method.

Important parts for the understanding of the project includes wind characteristics and interference with the turbine; building standards and codes; load and resistance factor design and also the materials / wood products that are to be used. Relevant global dimensioning loads are identified and considered in the structural strength capacity verification. An analytical initial scantling tool is established based on a cantilever beam model and implemented in MATLAB, thereafter verified with a shell model of the tower using the general purpose finite element software ANSYS. Sufficient dimensions of the tower cross sectional elements are derived for given circumstances of a future location of the tower. The strength calculations are made in ultimate limit state and the deformation analysis in serviceability limit state. Furthermore the first natural frequencies of the tower are verified to not coincide with the rotor frequency and the blade passing frequency of the turbine during operation, as well as the risk of vortex shedding. The dynamic analysis is carried out in FAST, simulating a turbulent and an uniform wind field. The thesis work shows that the simple beam model is a good candidate for conceptual design of wind turbine wooden towers.

Acknowledgements

I would like to thank my supervisor and examiner Mats Ander for all guidance and support during the master thesis. Furthermore, I would like to thank Håkan Johansson who introduced and assisted with the FAST simulations, as well as helping with his knowledge in discussions. I would also like to thank Otto Lundman, Joakim Örneblad and David Olivegren at Modvion for giving me the opportunity of working with this project and for providing with encouragement.

Table of Contents

Abstract	i
Acknowledgements	iii
Table of Contents	vi
1 Introduction	1
1.1 Objective	1
1.2 Baseline concept	1
1.3 Limitations	2
1.4 Method	3
2 Wood as Construction Material	4
2.1 Mechanical Characteristics	4
2.2 Glued Laminated Timber	6
2.3 Laminated Veneer Lumber	7
2.4 Material Properties	7
3 Design Criteria	8
3.1 Load and Resistance Factor Design	8
4 Loads	10
4.1 Wind load	11
4.2 Rotor Thrust Force	15
4.3 Rotor Torque	16
5 Analytical Model	19
5.1 Beam Model	19
5.2 Load Configuration and Strength Capacity	20
5.3 Deflection	21
6 Finite Element Model	22
6.1 Geometry	22
6.2 Element Types	22
6.3 Material Properties	22
6.4 Loads and Boundary Conditions	23
7 Dynamic Model	24
7.1 Wind Simulation with Interacting Turbine	24
7.2 Excitation Problems	27
8 Results	31
8.1 Analytical Results	31
8.2 FEM Results	39
8.3 Dynamic Results	42
9 Discussion and Conclusion	52
References	I

Appendix	III
Appendix A: Dynamic Analysis	III
A1. Input properties FAST	III
A2. Vortex Frequencies	IV

1 Introduction

As the wind power towers grows taller and wider there has appeared transportation problems of large parts to the site, due to the road regulations. Modvion develops a modular design of wind power towers made out of wood. The concept provides an advantage concerning transportation and assembly, which results in a possibility to build higher towers as well as lowering cost and a reducing CO₂ emission. Through taller wind towers it is possible to exploit energy harvest in areas which has not yet been utilised. The aim is to eventually produce towers that can be located in for instance a wood landscape, where it would not interrupt proximity's. The tower would reach above the treetops in order to attain the wind. Compared to conventional steel (and/or concrete) towers it would be a benefit in the environmental aspect, due to the demanding considerable resources and energy consumed during the production of traditional construction materials. Another favourable fact is that timber products are lighter which is an advantage not only during the transportation, but also during the assembly since it requires fewer and lighter lifts through machine capacity.

However, since the company at the moment is in the initial stage of the development, the intention is to primarily achieve a smaller model than the intended final version. Thanks to their contacts, a prototype in a smaller scale will therefor be build, located in the cost area of the municipality of Gothenburg. Nonetheless, in this project the intended full scale model will be considered in order to verify the conceptual design in combination with the dimensions and the capacity of the materials that are to be used. Modvion is currently as mentioned at an early stage in the business development, hence it is substantial to obtain a simplified model of the tower in order to reach an initial basic design considering the tower dimensions. This thesis work intend to identify basic scantlings and create a foundation for further static and dynamic analysis of the tower structure.

1.1 Objective

The objective of the thesis work is to carry out an initial analysis and strength verification of the tower structure to verify the load bearing capacity of the tower. The project includes analytical and finite element strength global analysis of the wind tower structure and determination of important dimensions of the cross section which influence the strength of the tower structure.

More specifically the aim is to identify loads in order to study the force flow in the tower. To set up and define initial analytic strength check, followed by an FE-model strength verification. This should be done using strength criteria according to relevant codes.

1.2 Baseline concept

Modvion has developed a baseline design of the modular tower concept and this section will give a brief overview of the prescribed tower geometry. The considered free standing tower is build up by several timber modules and has a conical shape, Figure 1. The details of the structure are classified and hence will not be demonstrated in the report. A simplified version of the structure is used in the calculations, which consists of an outer and inner panel connected with 32 supporting beams. A conceptual sketch of the cross section is shown in Figure 2. Moreover, the outer and inner sections are composed of a set of plates which are connected to constitute the total thickness of the walls. Walls are made of Laminated Veneer Lumber (in short form LVL, see Section 2.3) plates and the

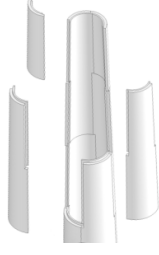


Figure 1: The modular design [9].

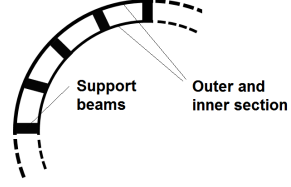


Figure 2: Conceptual cross section.

internal beams consists of Glued Laminated Timber (in short form GLT, see Section 2.2) beams. The aim is to investigate sufficient thickness of the walls in combination with a favorable dimension of the bottom diameter of the tower. Thickness constraints of the produced timber materials are 24 mm for the LVL and the cross section of the GLT beams are set to 405x215 mm. Thus, the thickness of the walls will be investigated in ranges of number of layers. The baseline proposal is to have three plates on the outside and two on the inside, which results in a thickness of 72 mm and 42 mm respectively. Furthermore a proposal of a base diameter is 11.5 m. Fixed dimensions of the tower are the top diameter of 4 m (due to the nacelle attachment) and the height of 120 m, as well as the dimensions of the GLT beams.

1.3 Limitations

The thesis work is carried out in collaboration with Modvion and by reasons of confidential information and agreements, details of the structure will not be included. The geometry is simplified and described above. Pre studies has been of importance in order to achieve a general knowledge and understanding of the research field of wind power technology. Many questions and speculations have been risen, although not all can be investigated since it is not in the scope of this project. Nevertheless it is good to have in mind, not least for future references.

Turbine simplification

In the design process of a wind power tower it is required to know for which wind turbine it is designed for including the type of generator, control method etc, since it affects the amplitude of the loads and hence the dimensions of the structure as whole [7]. Data from plant manufacturer, where requirements and specification of components are stated, are difficult to attain. By reason of lack of these data, there will be a simplification of the tower head induced loads. Throughout the pre-studies it has been decided to use data from an 5 MW reference wind turbine [1], developed by the National Renewable Energy Laboratory (NREL) and the National Wind Technology Center (NWTTC).

The significant loading on the tower are the resulting forces and moments from the rotor acting on the tower [7], hence only these are considered in the calculation. However, the inertial moments from the parts of the tower head influence the oscillation of the tower. In reality, the components have an elastic response causing imbalances due to stochastic loading, but aerodynamic unsteady loads on the turbine is beyond the scope. Hence, the including components of the tower head are considered as a rigid mass located at the top of the tower. Figure 3 shows the involved main components.

Foundation

Foundation of the tower is not included in the work. In the design process it is assumed that the tower is fixed in translation.

Long term effects

Long term effects within the material, such as creep and shrinkage will not be considered. Fatigue loads will not be in the scope of this project, since it will require more details regarding the connection design of the panels.

1.4 Method

The main part is to establish an initial analytic strength check which determines the initial dimensions of the tower. Calculations are made in MATLAB where the dependent parameters are altered to find appropriate dimensions for the variables that are examined. Feasible assumptions of the loads are identified and additionally by adopting strength criteria according Eurocode to meet the design requirements in structural building standards. Analytic calculations are followed by a FE-model analysis verification. The static structural modelling is performed in ANSYS. A dynamic analysis is done using FAST, where the tower interaction with the turbine is simulated, in order to check the magnitude of the thrust and torque. This is followed by a frequency control to verify that the turbine rotor speed is not operating in or close to the tower first natural frequency and at last an elementary check of the risk of vortex shedding problems.

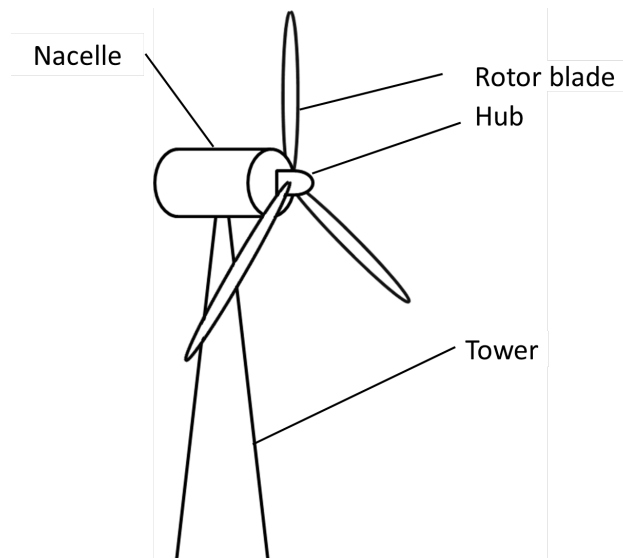


Figure 3: Principal sketch of main components.

2 Wood as Construction Material

Engineered wood products (EWP) is the notion of different fabricated timber products, joined together with for instance adhesives to form composite materials. With appropriate treatment and production method it is possible to take advantage of the mechanical properties and influence them. This chapter presents a brief preview of wood as a construction material, followed by a description of the two wood based structural products "Glued Laminated Timber" and "Laminated Veneer Lumber", which are the materials that are used in the tower structure. The material properties are specified in Table 1 the characteristic strength values in Table 3.1.

2.1 Mechanical Characteristics

Wood is a natural material that has been used in construction for centuries. It has been used in engineering and architecture systems due to its impressive durability and performance and is today one of the three most commonly used construction materials along with steel and concrete. In comparison to other construction materials, wood produces less carbon dioxide emissions in the manufacture of timber products. Further more it stores 700 kg airborne CO₂ per cubic meter which makes it a sustainable resource, [3]. The mechanical properties varies depending on the species, growth, production and treatment. Especially noticeable among timber products is the high strength capacity compared to the weight and the ability to transfer tension and compression. Additionally wood is a good insulator against heat and sound and is also easy to shape and detail to convenient size for the purpose.

Wood is an anisotropic material, which means that the mechanical properties are different in each direction in the material. This is due to the nature of the cell structure since it is composed of fibres aligned in the trunk. Figure 4 shows the coordinate system for a specimen where the fibres are oriented in the longitudinal direction denoted L. The trunk is regarded as almost circular symmetric in the symmetry plane. It is conventional to indicate the mechanical properties in the longitudinal, radial and transverse direction to the grains called the L- and R-/T-direction. Properties in the radial and transverse directions differ a lot from the longitudinal direction, tension strength in the parallel direction can be 30-50 times higher than in the perpendicular direction, [15]. Also the compression strength parallel to the grains are higher than in the perpendicular direction.

However, due to the nature of the material, growth defects appear which has an influence in the mechanical properties, [16]. Knots, uneven grain slope, moisture content, temperature to mention a few characteristics that affects. Presence of knots are a significant factor to consider since it reduces the strength. Size and shape, as well as where and how frequent it occurs decides how severe it will affect the character of the material. In production it is common to perform regularly tests during production of the wood material in order to control and classify the quality of the product. Within the European region a strength grading system for certification of timber products, called CE-marking, is used according to certain direction and rules.

An other important parameter that influence the product is the moisture content, especially in the perpendicular direction, [15]. It induces strain which will cause shrinkage when the moisture content is low and swelling when it is high. Therefor it is essential to be conscious of the moisture level, which often is measured both in dry and humid state.

During the growing period the tree is 100 % saturated with water and once cut and dried it reduces to 12-15 %, [12]. However, the moisture level is constantly changing depending on its surrounding. The values of the characteristic values in this thesis that are used are the so called 5th values. They are derived from test results of a specimen, during 5 minutes at the equilibrium state of moisture content, situated in a room temperature of 20 ° with a relative humidity of 65 %, [12]. The characteristic values are often used in static structural design of timber construction. From these values partial coefficients which are used in load and resistance factor design, further discussed in Section 3.1, are computed.

Furthermore, the quality of the timber is influenced by its surroundings and climate during the growth period, as well as the grow pace that at specific specie has. By looking at the width of the annual rings it is possible to see how fast the tree has been growing. Fast growing trees carry off wider rings which yields weaker wood with lower density.

An other interesting thing to notice is which part of the trunk that is used in the timber product, since the density vary along the tree. Additionally the cutting pattern, i.e. angle, size and location of the specimen determines the strength and its characteristics. Figure 5 illustrates how different parts of the trunk are cut and how the annual rings are located in the cross-section. Different parts are used for different purposes. Typically used for a higher classified materials is the part radial cut, since it is less effected of moisture movement in the material, and hence less responsive to shrinkage and swelling. It is the part where the variation in shape becomes the least.

The production of both GLT and LVL in Sweden is certificated by the SS-EN 14080 standards, which is the system to divide the different strength classes. While sorting the sawn goods it is also categorised by the amount and size of knots, cracks and other defects. The matter of fracture behaviour in wood products is complex, not only due to the composite configuration, but also as a result of the organic material. Traditionally crack growth, for more commonly used materials such as steel, is not thoroughly suitable for wood products and currently the understanding of the perpendicular grain failure is not specifically recognised, [15]. Fracture is not included in the thesis, but good to be aware of.

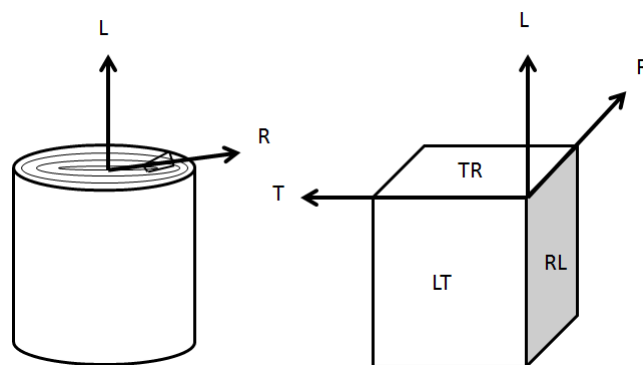


Figure 4: Coordinate system in wood.



Figure 5: Illustration of different cutting pattern of a wood trunk.

2.2 Glued Laminated Timber

Glued laminated timber (GLT, also called glulam) is a product which are produced by bonding several layers together with glue into one section. The technique results in higher strength and stiffness properties in the element as whole, than in solid wood and it also gives possibility to produce specimens in desired shapes, sizes and lengths. When using several numbers of layers, the defects are spread out. GLT as a construction material is more environmentally friendly since the energy used in production is lower than for other materials. It also causes low waste compared to using solid wood, considering that one can make use of the material resource more efficient and create products independent on the dimensions of the trees. In the manufacturing process a finger jointing technique is used to merge elements together lengthwise and thereby it is possible to produce boundless lengths of beams. Transportation, administration and assembly sets the limit of how large the timber beams can be made. Moreover the adhesive that is used in the jointing is synthetic glue, which constitute less than 1 % of the total weight of the final product, considered as negligible. In the manufacturing process of the wood product, the wood trunk is dried to a moisture content of 6-15%, which affects the mechanical properties. When a product with a lower moisture content is loaded by force it yields less camber and torsion.

The timber material that is to be used in the wind tower for the mid section beams is named GL30c, where the number 30 denotes the characteristic strength value (in MPa) and the c stands for combined. Moreover it means that the cross section consists of laminates of different strength classes. The outer zone, where the stress levels are highest, is composed of panels of higher quality than in the inner zone. The two outermost zones should not be larger than 17 % of the total height of the specimen. All layers in the cross section is oriented in the same direction.

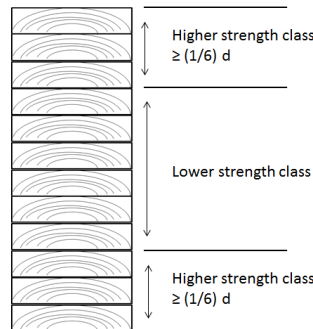


Figure 6: Illustration of the layers in GLT.

2.3 Laminated Veneer Lumber

Laminated Veneer Lumber (LVL) is produced by joining veneer sheets together, conceptually illustrated in Figure 7. The timber is similar to a plywood sheet. As for the GLT the highest graded sheets are placed in the outermost faces. Lay-up configuration of the cross-section decides the characteristics of the element and there are many options. The veneer sample that is to be used for the inner and outer shells of the support structure is 24 mm thick and will be jointed together to form a thicker frame. For further interest the lay-up for the specific LVL product from the supplier is constituted by three parallel sheets followed by one perpendicular.

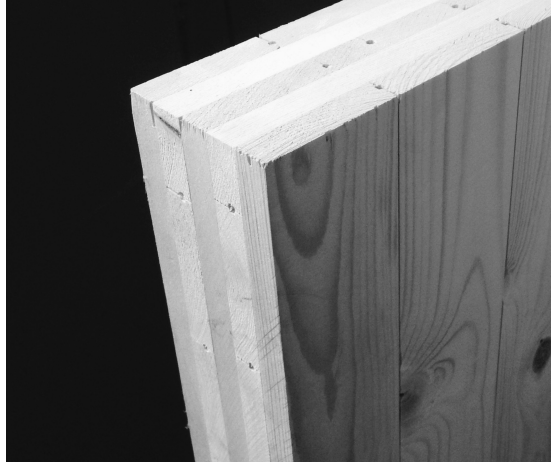


Figure 7: Conceptual illustration of the layers in a LVL plate.

2.4 Material Properties

The two considered wood products LVL and GLT have a 3D orthotropy illustrated in Figure 4 and the materials are regarded as homogeneous. The material properties are shown in Table 1, taken from [3].

Table 1: Material properties

Property		LVL_{ULS}	LVL_{ULS}	GLT_{ULS}	GLT_{ULS}
Young's Modulus [MPa]	L	8300	10000	10800	13000
	R	1000	1200	250	300
	T	100	130	250	300
Shear Modulus [MPa]	LR	400	600	540	650
	RT	16	22	54	65
	LT	60	60	540	650
Poisson's Ratio [-]	LR	0.2		0.5	
	RT	0.35		0.33	
	LT	0.45		0.5	
Density [kg/m^3]		510		480	

3 Design Criteria

3.1 Load and Resistance Factor Design

This section treats the reliability of a construction according to the European standard SS-EN-1990. It refers to the requirements in the ultimate limit state (ULS), with a method where statistically determined partial safety factors are applied accordingly to the design values for loading actions and material properties, [3]. It should be verified that the design resistance R_d is larger than the load effect E_d for the structure, i.e.

$$R_d > E_d. \quad (1)$$

The design value of the load effect includes permanent actions G and time-variable actions Q , which are combined to represent the comparable design situations. In Equation 2 the general formula for the load combinations is stated. Note that the declared "accidental" loads are not considered in the following.

$$E_d = \sum_{j>1} \gamma_{G,j} \cdot G_{k,j} + \gamma_{Q,1} \cdot G_{k,1} + \sum_{i>1} \gamma_{Q,i} \cdot \psi_{0,i} \cdot Q_{k,i} \quad (2)$$

Permanent loads are for this specific structure defined as the self weight from the tower and machinery and the wind action on the tower, rotor thrust and rotor torque are regarded as variable short term loads, which are accumulated during less than a week. They are all considered as variable main loads, since they are correlated to one another and acting simultaneously. The classification of the loads, depending on the duration, are determined according to SS-EN 1995-1-1, [4, Table G-2]. Load combination factors Ψ are decided according to [4], shown in Table 3.

Design values for load-bearing capacity

The design load in ULS is calculated acc. to STR-2 (STRength), where $\gamma_d = 0.83$ (safety class 1) is multiplied to each load variable, [3].

Table 2: Combination rules for load-bearing capacity in ULS acc to STR-2

Load	Load combination STR-2
Permanent loads G	
Unfavorable	$\gamma_d \cdot 1.2 \cdot G_k$
Favorable	$1.0 \cdot G_k$
Variable loads Q	
Main load $Q_{k,1}$	$\gamma_d \cdot 1.5 \cdot Q_{k,1}$
Combined variable loads ($\Sigma \cdot \Psi_{0,i} \cdot Q_{k,i}$)	$\gamma_d \cdot 1.5 \cdot \Psi_{0,i} \cdot Q_{k,i}$

Table 3: Load combination factors Ψ

	Ψ_0	Ψ_1	Ψ_2
Wind load	0.3	0.2	-

Design values for resistance

The design value of the design resistance is calculated for service class 3, which corresponds to an average moisture content for most softwood species exceeds 20 %, i.e. the structure is located unprotected outside. It is adjusted by the modification factor denoted as k_{mod} [3][Table 3.2]. The partial coefficients for the materials in ultimate limit state denoted as γ_M [3][Table 3.1], modification factors and characteristic strength values denoted as f_k [3][Table 3.4 and 3.6] for the two materials are summarised in Table 3.1. The calculated stress in the analytic model is derived from the resulting bending moment, hence the load effect is compared with the characteristic strength in bending denoted $f_{k,m}$ [3][Table 3.4 and 3.6].

$$f_d = \frac{k_{mod} \cdot f_k}{\gamma_M} \quad (3)$$

Table 4: Characteristic values for LVL and GL30c [3]

	$f_{k,m}[MPa]$	$\gamma_M[-]$	$k_{mod}[-]$
GL30c	28	1.25	0.7
LVL	30	1.2	0.7

4 Loads

This section will provide a review of the loading on the tower and present the contrived assumptions of the static design loads. Mathematical definitions of the identified variable and permanent loads are described in the following including:

- Wind actions on the tower
- Rotor -thrust and -torque
- Gravity load of tower and machinery.

Figure 8 shows the outline of the assumed load case. The analysis of the structural design will cover the basic global loading on the tower narrowed down to arrive from three sources, which are the wind q_w acting directly on the tower, the thrust F_{th} and torque M_T arriving from the aerodynamic loads on the tower head and the gravity load which includes the dead weight of the tower F_{tow} and the machinery F_{head} . There are several issues to take in to account regarding aerodynamic load on the tower head, since it is also interacting with the other sub -systems and -components in the nacelle, which influence the global loading of the tower. As already stated in the section regarding limitations a simplification is made. According to [6] it is explained that the loading arrived from the turbine house can be focused on the rotor, since it contributes the most significant wind actions.

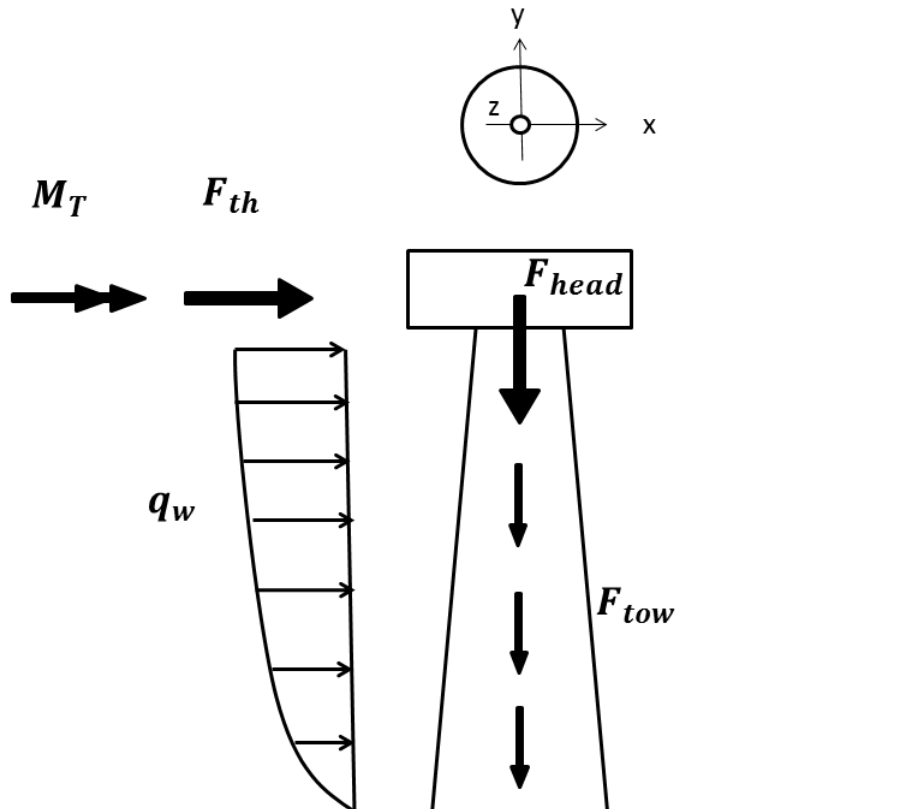


Figure 8: Applied design loads on the tower.

4.1 Wind load

The wind load is simplified to a static load where the flow direction is horizontally distributed on the structure. Nevertheless, the dynamic wind movement included by a turbulence factor, is covered in the formulas stipulated in the Eurocode [14]. A wind profile is produced by adopting these regulations and guidelines, which also consider the site specific environment in which the tower is presumed to be located in.

Wind characteristics

Wind passing a building causes the wind to break and the kinetic energy is transformed into potential energy of pressure, which generate the wind load [13]. Movement of the wind is also affected by surrounding topography. The wind is composed of a static component (mean wind) and a dynamic component (turbulence) due to stochastic rapid velocity changes. Wind speed increases with height as it approaches a structure. Created velocity pressure is based on a reference design wind speed, constituted by the mean velocity in 10 minutes at a reference height 10 m above the ground. The wind velocity variations can be said appearing in return periods, settled by the probability of occurrence. Extreme wind conditions is by custody measured in a 50 years return period, [13]

Wind actions according to Eurocode

When estimating the wind profile, i.e. the external wind pressure, the geographical location has to be considered. The following sections contain the calculation of the wind pressure on the tower according to the national standards in Eurocode (EN 1991-1-4 [14]). It contains guidance for the estimations and design criterion of wind actions used in structural design and the model includes dynamic response in the along wind direction.

The wind pressure acting normal to the tower surface is defined in Equation 4 and the including parameters will be briefly presented in the succeeding. For deeper explanation see the referred literature [14].

$$w_e(z) = q_p(z)C_{pe} \quad (4)$$

where

w_e	external wind pressure [N/m ²]
q_p	peak velocity pressure [N/m ²]
C_{pe}	pressure coefficient for external pressure
z	reference height [m]

The advice in the Swedish National Annex [4] is to calculate the velocity pressure according to Equation 5, where the reference wind speed, specifically determined for the considered municipality should be implemented. It is represented by the mean wind speed during a 10 minute period, 10 meters above ground for a 50 years return period. The roughness length is set to $z_0 = 0.05$. For the studied tower structure a reference wind speed of 25 m/s is selected, that is defined for the Gothenburg region stated in the Swedish National Annex [4]. One should note that the orthography factor (which is normally included in the international standard equation for the velocity pressure) is already taken into account while using the national recommendations. Additional consideration regarding the wind tower location it is appropriate to use terrain category II, which is describes as "Area with low vegetation such as grass and isolated obstacles (trees, buildings) with separations of at least 20 obstacle heights" [14].

$$q_p(z) = [1 + 6I_v(z)] \cdot \left[k_r \ln\left(\frac{z}{z_0}\right) \right]^2 \cdot q_b \quad (5)$$

$$q_b = \frac{1}{2} \rho_{air} v_b^2 \quad (6)$$

$$k_r = 0.19 \cdot \left(\frac{z_0}{z_{0,II}} \right)^{0.07} \quad (7)$$

where

- $I_v(z)$ turbulence intensity at height z , stated in Equation 8
- k_r terrain factor, stated in Equation 7
- q_b basic velocity pressure, stated in Equation 6, [N/m²]
- ρ_{air} air density [kg/m³]
- v_b basic wind velocity [m/s]
- z_0 roughness length [m]
- z_{min} minimum height [m]
- z_{max} to be taken as 200 [m]
- $z_{0,II}$ roughness length in terrain category II [m]

The including turbulence is treated in the equation of the peak velocity pressure as a turbulence intensity factor defined in Equation 8. It is based on the standard deviation of the turbulence and the mean wind velocity. Recommended value for the turbulence factor is $k_I = 1$ and the orthography factor is to be taken as $c_0(z) = 1$ as well.

$$I_v(z) = \frac{k_I}{c_0(z) \cdot \ln(z/z_0)} \quad \text{for } z_{min} \leq z \leq z_{max} \quad (8)$$

$$I_v(z) = I_v(z_{min}) \quad \text{for } z < z_{min} \quad (9)$$

where

- k_I turbulence factor
- $c_0(z)$ orthography factor

The external pressure coefficient, defined in Equation 10, is dependent on the geometry and size of the structure. In order to find an appropriate value, the aerodynamics of the circular cross-section must be considered, as the tower is regarded as a cylinder.

$$c_{pe} = c_{p,0} \cdot \Psi_{\lambda\alpha} \quad (10)$$

where

$c_{p,0}$ external pressure coefficient without free-end flow
 $\Psi_{\lambda\alpha}$ end-effect factor defined in Equation 11

The end-effect factor varies depending on the location of the surface, illustrated in Figure 9, as the wind approaches the cylinder. It is varying correspondingly to the flow separation which is characterised by Equation 11.

$$\Psi_{\lambda\alpha} = 1 \quad \text{for } 0^\circ \leq \alpha \leq \alpha_{min} \quad (11)$$

$$\Psi_{\lambda\alpha} = \Psi_\lambda + (1 - \Psi_\lambda) \cdot \cos\left(\frac{\pi}{2} \cdot \left(\frac{\alpha - \alpha_{min}}{\alpha_A - \alpha_{min}}\right)\right) \quad \text{for } \alpha_{min} < \alpha < \alpha_A \quad (12)$$

$$\Psi_{\lambda\alpha} = \Psi_\lambda \quad \text{for } \alpha_A \leq \alpha \leq 180^\circ \quad (13)$$

where

α_A position of flow separation [°]
 Ψ_λ end-effect factor

Furthermore the pressure coefficient depends on the Reynolds number stated in Equation 15, which is determined as 10^7 . In order to obtain the external pressure coefficient, the integral in Equation 14 must be evaluated, between the boundaries around half the circular surface representing the reference area on which the pressure acts.

$$c_{pe} = \int_0^\pi c_{p,0} \cdot \cos(\alpha) d\alpha \quad (14)$$

$$Re = \frac{b \cdot v(z)}{\nu} \quad (15)$$

where

b diameter [m]
 ν kinematic viscosity of the air [m²/s]
 $v(z)$ wind peak velocity [m/s]

Figure 9 illustrates the variation of the pressure coefficient around a cylinder. The graph of the variation of C_{pe} found in Eurocode [14] is reproduced by a curve fit in MATLAB, illustrated in Figure 10, whereas the integral is evaluated, resulting in $C_{pe} = 0.6129$. Inserting all parameters stated above and integrating along the tower height, provides the wind profile. Illustrated in Figure 21 is the external wind pressure on the tower according to Equation 4.

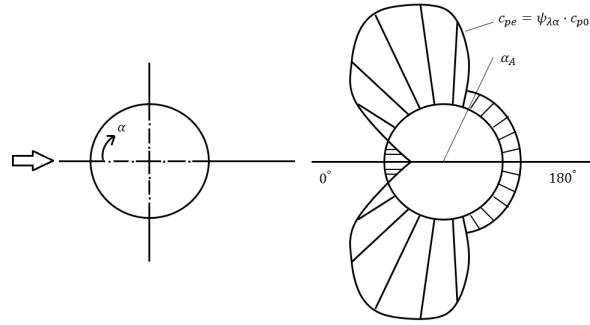


Figure 9: Illustration of the pressure coefficient around a cylinder.

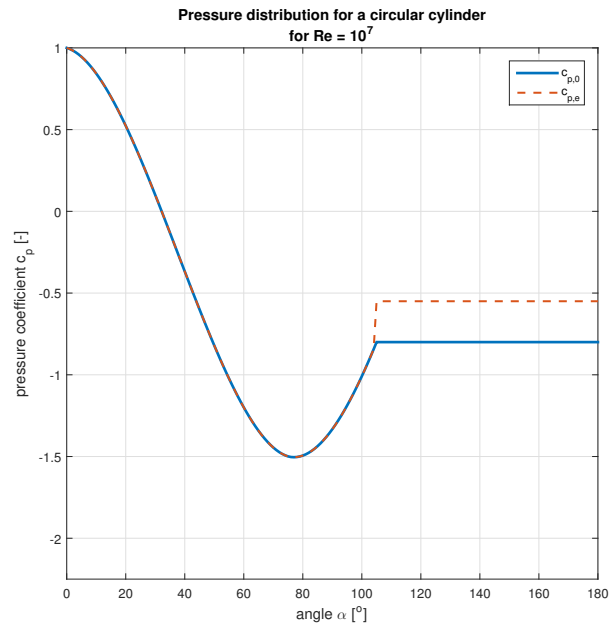


Figure 10: Pressure coefficient around a cylinder (for $Re = 10^7$) according to MATLAB curve fit.

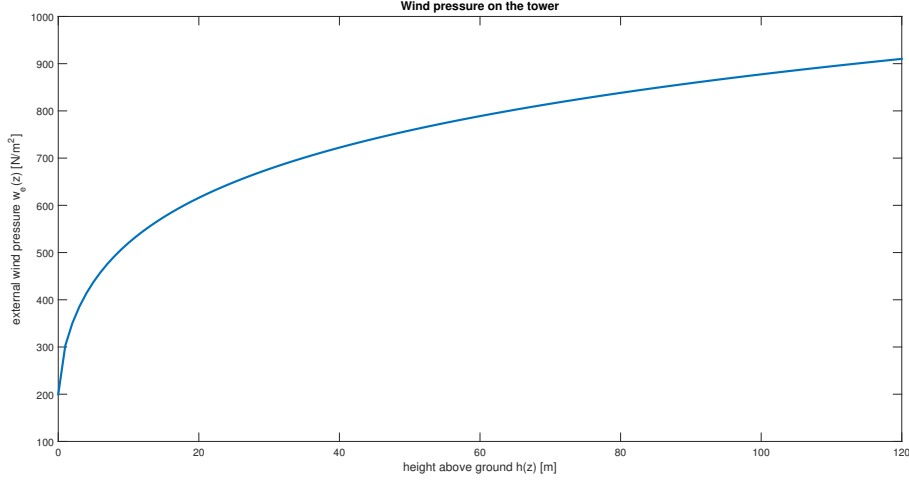


Figure 11: Wind pressure distribution.

4.2 Rotor Thrust Force

An approximation of the rotor thrust F_{th} is made as a static horizontal force applied at top of the tower, stated in Equation 16.

$$F_{th} = -\frac{1}{2}\rho_{air}C_TA_{rd}u_{rot}^2 \quad (16)$$

where

- A_{rd} rotor disk area [m²]
- C_T thrust coefficient
- ρ_{air} air density [kg/m³]
- u_{rot} average wind speed over the rotor [m/s]

The thrust coefficient C_T is dependent on many factors, mainly the geometry of the blades, the tip speed ratio (TSR) and pitch angle. Equation 17 formulates the definition of the TSR, also denoted as λ . However, since the coefficient is a function of many variable parameters it is convenient to determine it by use of a wind tunnel simulation. Due to this fact and also in consideration of the unknown design geometry and data specification of the turbine blades and their response for different wind speeds, an approximation has been made based on basic formulas. The approximation is based on the steady-state response of the land-based 5 MW turbine, defined by the National Renewable Energy Laboratory (NREL) [1]. Measured data, shown in the graph in Figure 12 and 13, are obtained after running a series of dynamic simulations at a couple of steady uniform wind speeds. It can be seen in Figure 12 that the rotor thrust is as largest during a wind speed of 11.5 m/s. Thus, this value is chosen to the standard formula in Equation 16, which corresponds to a TSR of 7 in Figure 13. Thereafter it is compared with the diagram in Figure 14, where the relation between C_T and TSR are shown. A TSR of 7 and pitch angle 0° corresponds to a $C_T = 0.75$.

$$\lambda = \frac{R\Omega}{u_{rot}} \quad (17)$$

Applying the values into Equation 16 results in a static thrust of 808 kN.

4.3 Rotor Torque

In the same manner the static rotor torque M_T , defined in Equation 18, is determined by the graph in Figure 15. For a TSR of 8 m/s and pitch angle 0° , the power coefficient C_P is 0.48.

$$M_T = -\frac{1}{2}\rho_{air}A_{rd}C_P u_{rot}^3 \Omega^{-1} \quad (18)$$

where

A_{rd}	rotor disk area [m ²]
C_P	power coefficient
ρ_{air}	air density [kg/m ³]
u_{rot}	average wind speed over the rotor [m/s]
Ω	rotor speed [rad/s]

Inserting these values results in a torque of 4.4 MNm.

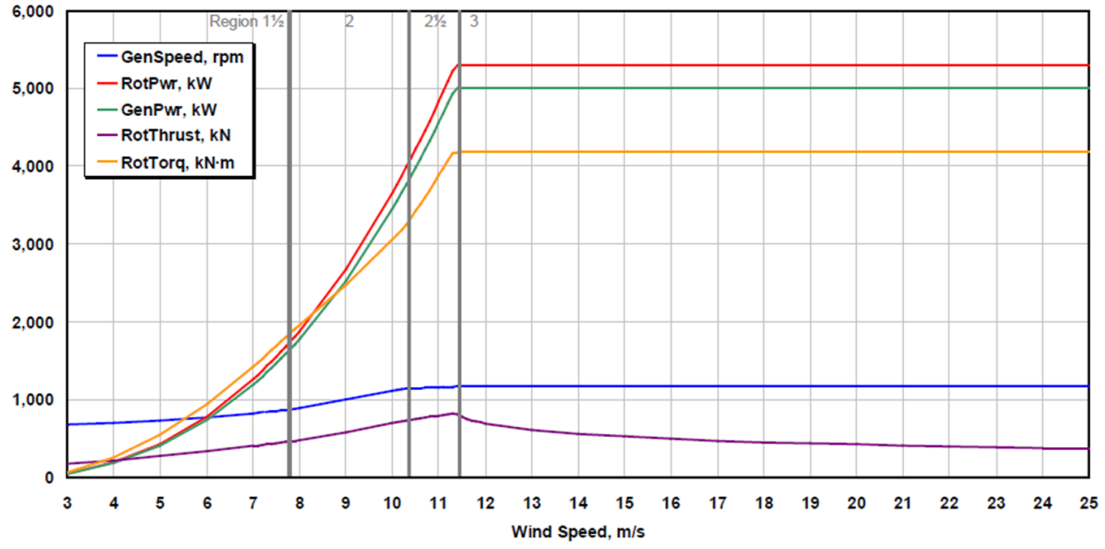


Figure 12: Relation between wind speed and the thrust- and torque- load for the NREL turbine, from [10]. *RotThrust* and *RotTorque* represents the rotor thrust and the rotor torque respectively.

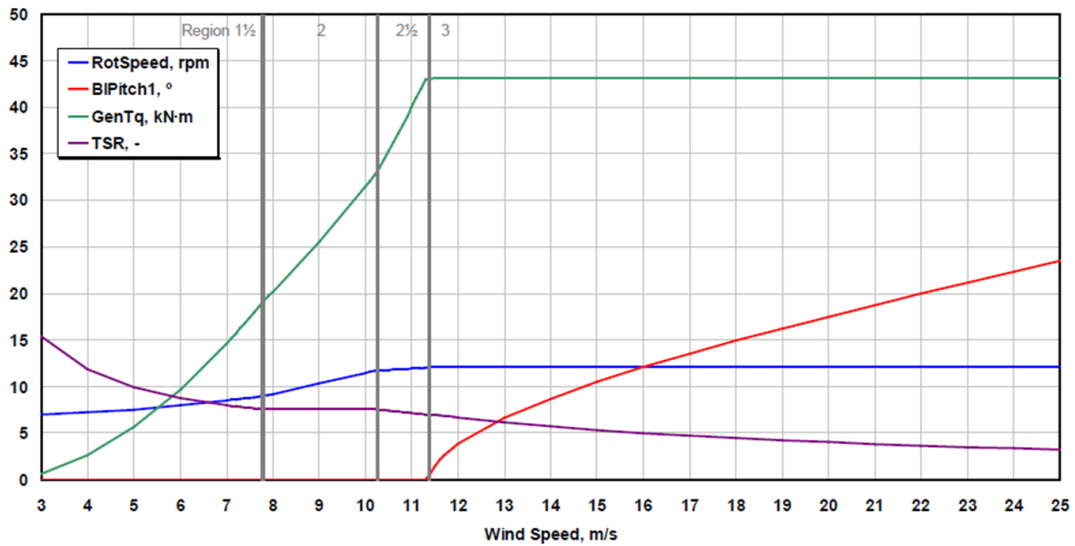


Figure 13: Relation between wind speed and the TSR for the NREL turbine, from [10].

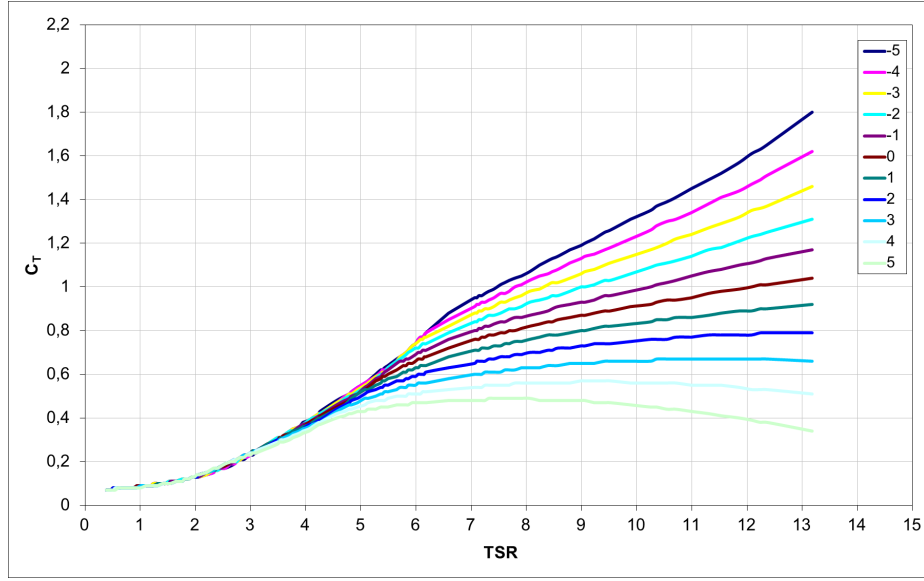


Figure 14: Relation between C_t and TSR for the NREL turbine, from [10].

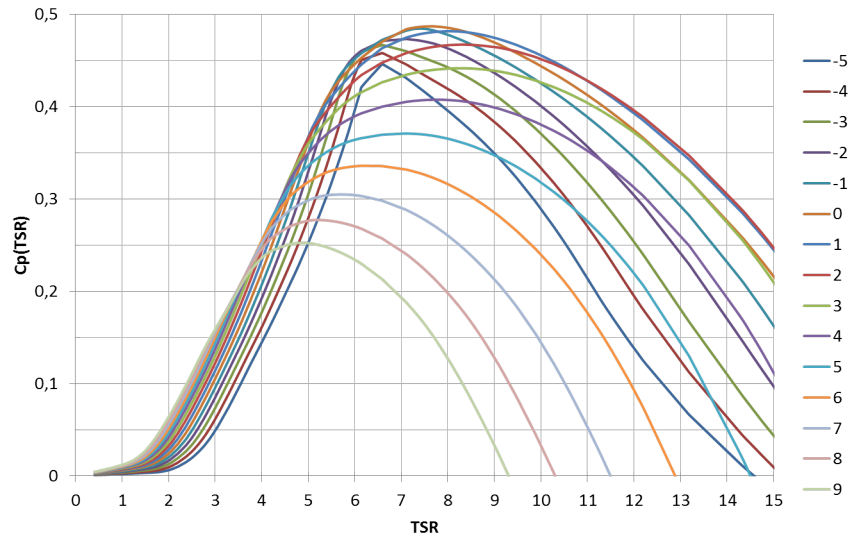


Figure 15: Relation C_p and TSR for the NREL turbine, from [10].

5 Analytical Model

The relation between the tower geometry and applied loads are analysed using an analytical model, where the stress distribution in the tower structure are studied for varying dimensions. Analytical calculations are performed in MATLAB using the Euler Bernoulli beam theory and the loads are defined according to Section 4 magnified with load factors described in Section 3.1 and compared with the design values of resistance.

5.1 Beam Model

Load capacity calculations are based on Euler Bernoulli beam theory, i.e. the structure is considered as a continuous beam and shear deformations are neglected. For thorough definitions of the Euler Bernoulli beam theory see e.g. [2]. The fundamental differential equation is stated in Equation 19. It represents the relation between a distributed load $q(z)$ and the deflection u perpendicularly to the z -axis of the beam.

$$q(z) = \frac{d^2u}{dz^2} \left(EI \frac{d^2u}{dz^2} \right) \quad (19)$$

Equation 20 defines the relation between bending moment M and deflection,

$$M(z) = -EI \frac{d^2u}{dz^2} \quad (20)$$

and the relation between a distributed load, bending moment and shear force are defined in Equation 21

$$\frac{dV(z)}{dz} = -q(z) \quad \frac{dM(z)}{dz} = V(z) \quad (21)$$

According to the Euler Bernoulli beam theory the total stress in the tower, aroused from several loads, is obtained by a summation of them. In total the experienced stress in the cross-section, due to bending and normal force, is defined in Equation 22. The stress is evaluated for the outer point of the structure where it is assumed to be largest, which correspond to the distance $D(z)/2$ from the neutral axis.

$$\sigma(z) = \frac{M_{xy}(z)}{I(z)} \frac{D(z)}{2} + \frac{N(z)}{A(z)} \quad (22)$$

Each load is calculated separately and then recalculated to the induced bending moment. Thereafter moments in x - and y -direction are summarised respectively and combined into one total moment, Equation 23.

$$M_{xy}(z) = \sqrt{M_x(z)^2 + M_y(z)^2}, \quad M_y(z) = M_w(z) + M_{th}(z), \quad M_x(z) = M_T(z) \quad (23)$$

In the analytic model the tower is regarded as being continuous and does not include the separate constituted modules. The circular cross section contains an outer and inner shell connected with 32 supporting beams with a rectangular cross section. Since the tower has a conical shape the diameter is varying along the z -axis with a defined bottom and top diameter. This means that the area and area moment of inertia is also varying with the

height. Due to the principles of the Euler Bernoulli model the loads are applied according to a 2D interpretation, in horizontal and vertical direction to the beam. The top diameter is fixed to 4 m by reason of the plant area between the tower and the nacelle, but the bottom diameter is to be analysed by adjusting it to stay within the acceptable range for the load-bearing capacity.

In detail the area moment of inertia for a plane region is determined by summing up all contributions from each segment of the cross section, by Steiner's parallel axes rule. For an annulus, with an outer diameter D_o and inner diameter D_i , it is defined as I_c in Equation 24. It is calculated for both the outer and inner segment. Contributions from the support beams are summed up as I_d in Equation 24, where A is the rectangular cross sectional area and d is the perpendicularly distance from the neutral axis of the global structure to the centre of gravity of each beam respectively. Note that the area moment of inertia around its own axis is neglected, since the contribution is significantly smaller than the one around the global y- and x-axis respectively.

$$\begin{aligned}
 I &= I_c + I_d \\
 I_c &= \sum_{n=1}^2 \frac{\pi}{64} \cdot (D_o^4 - D_i^4) \\
 I_d &= A \sum_{n=1}^{32} d^2
 \end{aligned} \tag{24}$$

5.2 Load Configuration and Strength Capacity

Figure 16 shows the coordinate system and the directions in which the loads are acting. The direct wind actions on the tower, determined in Section 4.1, is distributed along the tower. Load due to self-weight of the tower distributed in z-direction, which is largest at the ground level, where the structure experience the most of the self weight. The steady loads which appear due to aerodynamically thrust act as the axial force in x-direction and the aerodynamically rotor torque act in same direction as the rotation of the rotor. Rotor thrust and torque are both considered to be transferred at the tower top, at the height of 120 m. It is noted that in reality these loads are enforced a bit further up located in the nacelle.

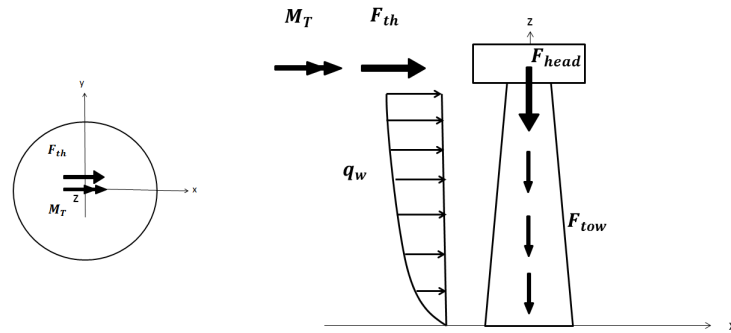


Figure 16: Applied design loads on the tower, above and side view.

Both the wind action load and the rotor thrust load contributes to the bending moment in y-direction and the torque in x-direction.

The bending moment in the structure due to the wind load described in Section 4.1 is obtained by Equation 25, where the wind pressure is transformed into a distributed load $q_w(z)$ by multiplying with the width of the projected area of the tower, i.e. the tower diameter. Once again it should be noted that this calculation is due to a 2D observation, where the drag coefficient C_d is a summation, which means the compression and tension are summarised along the periphery.

$$M_w(z) = - \iint q_w(z) \, dzdz, \quad q_w(z) = w_e(z)D(z) \quad (25)$$

Contribution from the axial rotor thrust is calculated by Equation 26

$$\sigma_{th}(z) = \frac{M_{th}(z)}{I(z)} \frac{D_o(z)}{2}, \quad M_{th}(z) = - \int F_{th} z \, dz \quad (26)$$

and the rotor torque applied at the top is acting distributed along the whole tower height resulting in the stress in Equation 27

$$\sigma_{M_T}(z) = \frac{M_T}{I(z)} \frac{D(z)}{2} \quad (27)$$

Stiffness correction

Since the two materials have different modulus of elasticity it has to be taken into account. The problem is treated as two dimensional and the plain cross section condition means that the two adjacent materials in the cross section will follow the same linear strain distribution. The second area moment of inertia for the supporting beams I_d and the area A_d should be multiplied with a factor E_{GLT}/E_{LVL} to compensate for the relation between the difference in elasticity modulus. Further the factor is also applied to the obtained resulting stress in the GLT material.

5.3 Deflection

The deflection at the tower top is calculated according to Equation 28, where the integration is performed in MATLAB. Results are presented in 8.1. The applied modulus of elasticity is the SLS value of the two materials, used in deformation calculations. The two components of the second moment of inertia are each multiplied by corresponding elastic modulus according to Equation 28.

$$w(z) = - \iint \frac{M_{xy}(z)}{EI(z)} \, dzdz = - \iint \frac{M_{xy}(z)}{E_{LVL_{SLS}} I_c(z) + E_{GLT_{SLS}} I_d(z)} \, dzdz \quad (28)$$

6 Finite Element Model

In order to verify the analytic calculations and compare the strength capacity of the tower structure, a FE-model is established in the commercial software ANSYS. Static strength capacity is studied for the implemented tower geometry. This section provides how the modelling is carried out, including the framework of the geometry, appliance of loads, boundary conditions, material parameters etc. Computational results are presented in Section 8.2.

6.1 Geometry

Input geometry variables are prescribed from the analytical model. All parts in the tower are modelled with shell elements which has their mid plane in the centre of the panelling. Outer and inner section are bound by the supporting beam connected by associated nodes. Due to the nature of the computer software there is an additional width of the beam in order to connect the parts correctly. However, this modelling inaccuracy is not affecting the result significantly since the increased texture is very small and considered as negligible in the consideration of the global analysis of the wind tower structure.

Considering the orthotropy of the materials, all parts of the tower (one outer wall, one inner wall and 32 stringers) are modelled with the element orientations in longitudinal, transverse and radial directions to be consistent with the material definitions. The materials of the wood products have 3D orthotropy are regarded as homogeneous.

6.2 Element Types

The tower structure is modelled with quadratic 2D shell elements that simulates the 3D geometry. A convergence study is made where two elements called SHELL181 and SHELL281 are compared. They have four and eight nodes respectively. Naturally it showed that the modelling with higher order of elements converged faster with less number of elements. The element type that is used is thus the eight node element, where each node has six degrees of freedom, translations in and rotations around x-, y-, and z-axes. The element is commonly used in analysis of thin to adequately thick shell structures.

6.3 Material Properties

ANSYS software claims more material parameters than in a model using Euler Bernoulli beam theory. It is required to define values for the shear modulus and Poisson's ratio. Furthermore, the difference between the 1D-model and the 3D-model is the definition of the material model in the FE formulation. In the analytic 1D beam model the elasticity is naturally only considered in one direction, while in the 3D-model it assumed that the material is orthotropic. This means that additional components are specified for three directions. Table 1 shows the implemented material data values.

6.4 Loads and Boundary Conditions

The total weight of the nacelle is applied as a point mass applied by a remote attachment in a point in the centre of the tower at 120 m height, see Figure 31. The remote point is connected to the nodes at all edges at the top. All dead weight bodies, the tower top mass and the including tower components, are influenced by the standard earth gravity specified to 9.8066 m/s^2 .

Thrust and torque experienced at the rotor are applied as remote loads in the same remote point aforementioned.

As previously mentioned the pressure (stated in Equation 4) from the inflowing wind is dependent on the external pressure coefficient (stated in Equation 10). In the analytical 2D model a summation of $C_{p,e}$ is used as an approximation, which means that the external wind pressure is only varying in z-direction. Nevertheless the end-effect factor is varying over the surface (along the periphery) and in the FE modelling this is implemented for a more realistic approach. Numerical values of the end-effect factor at 181 points in the circumference are calculated for each meter of the tower height, i.e 121 points in z-direction. Consequently 21 901 data values are achieved in order to realise the wind pressure in two directions. The load vector is imported in ANSYS which utilise external data appearing in an approximation where the software generate an interpolation which ends up with pressure values for each node. The mapping of the calculated data results in a difference, as the values of the pressure is slightly different in the bottom and top of the tower. Pressure is applied at the corner nodes of each element normal to the surface of the outer wall. The distribution of the load is shown in Figure 17.

The structure is constrained at the bottom edges. Moreover it is restricted to be fix in translation in three directions but allowed to rotate.

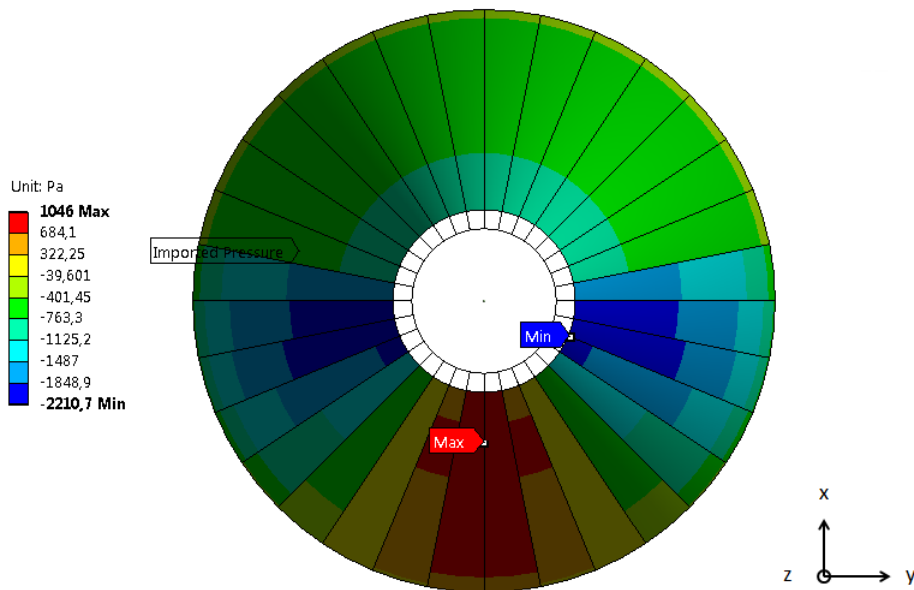


Figure 17: Applied pressure in ANSYS.

7 Dynamic Model

The analytical analysis of the tower is based on permanent static and quasistatic dynamic loads, where the thrust and torsion at the top of the tower head are calculated based on extracted data from the specification of a baseline turbine, developed by NREL (National Renewable Energy Laboratory, U.S.) [11]. Thus a dynamic model is established in order to verify the accuracy of the applied static loads.

Dynamic simulations which includes the planted turbine are performed using FAST (Fatigue, Aerodynamics, Structures and Turbulence) which is a multiphysical engineering tool developed by the NWTC (National Wind Technology Center).

For the load bearing capacity of the support structure, it is of interest to compare if any of the crucial frequencies of excitation is close to the natural frequency of the tower, which would increase the resulting response load and give higher stresses in the tower. Critical concerns that are essentially controlled in the development of a wind turbine support structure are the rotor frequency and risk of any vortex shedding actions, that might cause severe damage if it coincides with the natural frequency of the tower.

7.1 Wind Simulation with Interacting Turbine ¹

The dynamic model includes a wind simulation of the support structure along with a reference turbine integrated at the tower top. The baseline wind turbine modelled with the engineering tool FAST includes all drive train properties and other structural parameters of the components in the nacelle head, the control and electrical system etc. It is not an existing turbine, but the conceptual model is commonly used in the area of wind technology in order to model the coupled dynamic response, since there are difficulties to achieve proper data from the suppliers. There are many modules included in the FAST tools, such as the aerodynamics, servo dynamics etc.

For the practice of this work, a land based reference turbine is used with a rated power of 5 MW. All properties and data is open for publicity and can be found in the technical report from NREL, [1]. It is a three bladed, horizontal, upwind turbine which is variable speed and variable blade-pitch-to-feather-controlled. The pitch control system adjusts nacelle and blades, so that they are rotated into the best pitch angle in the interest of gaining the largest energy harvest, which is directed towards the inflowing wind. Each wind turbine has a specific cut-in wind speed, which is the minimum for the turbine to start rotating. When reaching this point the blades turns into position and power generation is activated. Furthermore, each turbine has a specific limit of the capacity where the generator has its maximum power output corresponding to the rated rotor speed and the rated wind speed. However, during too high wind speeds and/or turbulence the control system regulates the blades or put the rotor on to a brake if necessary. This occurs at the cut-out wind speed in order to avoid damage of the turbine and tower. Table 5 specifies the wind and rotor speed data for the reference turbine used in this work.

In the simulation a pitch angle of 0° toward the wind is used, where the largest forces on

¹Late in the process of the thesis work a correction of the calculations were pursued, which affected the tower eigenfrequencies. All calculations and results carried out with the FAST tools are therefor reported with the old values. The first and second tower eigenfrequency changed from 0.29197 Hz and 1.1544 Hz to 0.29849 Hz and 1.731 Hz respectively. The updated adjustments resulted in a stiffer tower structure which increased the frequencies slightly.

Table 5: Specifications of NREL 5 MW baseline turbine

Wind speed [m/s]	cut-in	3
	rated	11.4
	cut-out	25
Rotor speed [rpm]	cut-in	6.9
	rated	12.1

the structure is experienced. Processing of the turbine is not treated in this work, only the module dealing with structural dynamics of the tower is used. The rotor diameter of the turbine studied is 126 m and the length of the blades are 61.5 m. The hub is located 122.4 m above the ground. Of interest is that the model of the turbine uses 16 degrees of freedom, in order to rotate the turbine aligned with the inflow wind. The modelling of the blades and tower uses a linear modal representation, where small deflections are assumed. Two bending modes in fore-aft as well as side-to-side for the tower and two flapwise and one edgewise bending mode for each of the three blades are adopted.

As mentioned above the intention with the time variable simulation is to verify the thrust and torque that is imposed to the tower head. Other parameters of interest that can be extracted from the dynamic simulation is the displacement at the top of the tower and the reaction force at the tower base. All though there are numerous different load cases and scenarios to be checked in a specific project work, a basic check is done when the wind turbine is operating in a turbulent wind field specified in accordance with a mean wind speed above normal.

Included in the binary data files from NREL are a couple of certification test cases that can be simulated. In this case "Test18" is used in the simulations. The configuration changes in the model, which originally is pre-defined for a modular steel tower, are the properties of the tower and the aerodynamic wind field. All turbine specific properties are left with their default values.

The input tower properties, height and diameter, are implemented for ten sections (eleven points) distributed along the tower. Values for the mass density and stiffness are shown in Table 11 in Appendix 9. The stiffness in the fore-aft and side-to-side are the same due to symmetry of the cross section geometry.

In order to run the simulation, it is required to apply input data for the first two mode shapes in fore-aft and side-to-side. Each mode is described as a 6th order polynomial expression, where the coefficients of term 2-6 must be prescribed. Relative location and deflection along the tower are achieved from ANSYS Modal Simulation. Thereafter a curve fit is made using MATLAB in order to achieve the polynomial equations of the modes, results are plotted in Figure 18. Considering that the structure is regarded as a flexible beam which is cantilevered from the ground where the deflection and slope are zero, it implies a boundary condition of term x^0 and x^1 equal zero. Tower height location and deflection are normalised to a value equal one regarding the tower top height and largest deflection respectively, such that the sum of all polynomial coefficients must add to one.

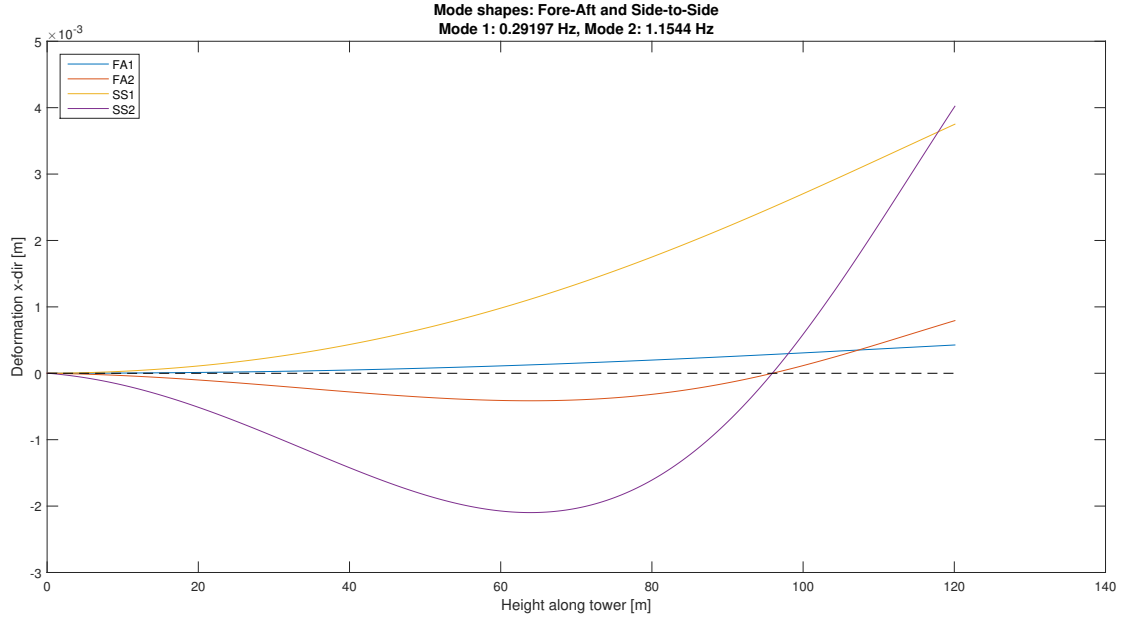


Figure 18: Mode shapes extracted from ANSYS Modal Simulation.

The wind field is generated by TurbSim which is a stochastic turbulent wind simulator that reads input text files. It executes three components of the fluctuating wind speed vectors, positioned in a two dimensional grid of 31×31 points that is fixed in space, [8]. The wind simulator determines the wind profile considering a characteristic mean wind speed of 12 m/s. Furthermore it is scaled with turbulence factors, where the characteristic of the turbulence is defined according to IEC standard for class B - medium turbulence with a value of 14 % intensity. All files with input data of the aerodynamics are left intact, except for the reference height of the horizontal wind speed which is changed to 120 m.

Simulations have been carried out for different initial rotor speeds, in order to see the the response in the structure during a start-up phase and also during operation. In the simulation files the time step is defined to be constant 0.00625 seconds. Initially the duration of the simulation was 60 seconds, but it appeared that it would take longer time for the rotor to reach the operational mode where the system is stabilised. Thus the simulation time was extended to 90 seconds in order to see the behaviour in the reaction and if any indications of vibration problems. Results for the signified cases are presented in Section 8.3. Additionally a simulation in a uniform wind field is performed, with a constant wind velocity at 11.5 m/s and a rotor speed of 12 rpm, which correspond to the values implemented in the static analytical model.

7.2 Excitation Problems

Calculation in this section is carried out with the updated data, i.e. after the error was corrected.

Interaction in Drivetrain-Tower System

A concern that is highly connected to the stiffness requirement of the wind turbine tower is to examine the tower natural frequency and the relation to the exciting frequency of the turbine, mainly influenced by the rotor frequency [7]. Commonly, the rotational frequency is referred to as 1P and the blade passing frequency for three blades to as 3P. A control is made to verify that the first natural frequency of the tower is within an allowable range, namely between 1P and 3P, to avoid resonance. If the frequencies coincides there is resonance there is a risk for excessive vibrations and possible failure of the structure. There is no accustomed safety distance from the critical frequencies, since there are different damping systems for different turbines and support structures, [6]. Requirements from reviewed literature suggests a variety of ranges that the tower natural frequency should be within, thus a check of $\pm 5\%$, $\pm 10\%$ and $\pm 25\%$ off 1P and 3P is confirmed.

Table 6: Allowed frequency ranges

	Critical Frequency Range	
	[Hz]	
	1P: 0.20167	3P: 0.605
$\pm 5 \%$	0.1916	0.5747
	0.2117	0.6352
$\pm 10 \%$	0.1815	0.5445
	0.2218	0.6655
$\pm 25 \%$	0.1513	0.4537
	0.2521	0.7562

According to the result from ANSYS, the first bending mode for the tower structure including the tower head mass is 0.29849 Hz. In normal operation the rated rotor speed is 12.1 rpm which means that the rotor frequency 1P is 0.20167 Hz and the blade passing frequency 3P is 0.605 Hz. Table 6 presents the critical frequency ranges, calculated for the three percentages. Comparing the values it appears that the first bending frequency of the tower lies within 1P and 3P.

In this context it should also be mentioned that structure is considered as "soft" design, hence there will be risk of resonance during start up and shut down, since the frequencies will for a short time coincide. The first tower bending frequency will coincide with the rotor frequency at corresponding 5.8394 rpm illustrated in Figure 19. This value is noted and further discussed in Section 8.3 where the turbine-tower response is observed. The first natural frequency must be passed quickly, in order not to develop large oscillations. Normally there is a control system to damp vibrations.

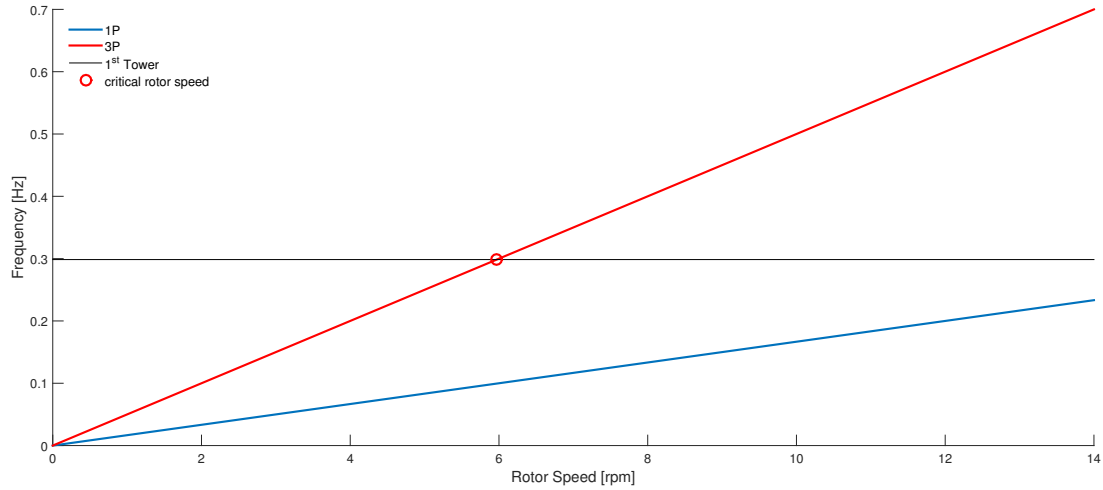


Figure 19: Critical Rotor Speed.

Vortex Shedding

Another structural vibration that may occur for a slender structure such as the considered tower is vortex shedding, if it coincides with any of the natural frequencies of the tower. Alternated vortices that are shed from two opposite sides of a structure may generate vibrations. This will induce a fluctuating load perpendicular to the wind direction and as the shedding of the vortices alternately slips from one side to an other, it causes a harmonic load with the same frequency as the vortex shedding ($f_{vortex}(z)$ Equation 29).

Prediction of vortex shedding is described as crude, since there are no fully developed analytical model for the phenomenon [5]. Analysis of the physical vortex shedding is mainly completed using computational fluid dynamics analysis. Eurocode 1 [14] comprises a proposition for predicting if vortex induced vibrations are present. Following the procedure stipulated in Eurocode 1 will indicate if there is a need for further provisions due to the vortex actions.

The frequency of the vortex shedding induced load is described by Equation 29

$$f_{vortex}(z) = St \cdot \frac{v_m(z)}{D(z)} \quad (29)$$

where

- St Strouhal number, $St = 0.18$ for a circular cross section
- $v_m(z)$ mean wind velocity, stated in Equation 30
- $D(z)$ cross section width, the outer diameter for the considered structure

$$v_m(z) = c_r \cdot c_o \cdot v_b \quad (30)$$

$$c_r = k_r \cdot \ln\left(\frac{z}{z_0}\right) \quad (31)$$

where

- c_r roughness factor, stated in Equation 31
- c_o orthography factor, taken as 1.0
- v_b reference wind speed, (25 m/s Gothenburg from the National Annex [4])
- k_r terrain factor, stated in Equation 7
- z_0 roughness length, (0.05 from the National Annex [4])

Calculating the vortex shedding induced frequency and comparing with the first and second natural bending frequencies for the tower (0.29849 Hz and 1.731 Hz), it appears that the first tower frequency coincide at around 4 meters height and no risk for the second tower frequency to coincide.

As a notation to the detected risk for development of large oscillations, it might necessarily not be a problem. By looking at the mode shape of the tower, the deflection due to the first bending frequency is not that large at the height four meters and hence is not likely to produce exaggerated vibrations. This is illustrated in Figure 20, where the deformation amplitudes and tower height are normalised.

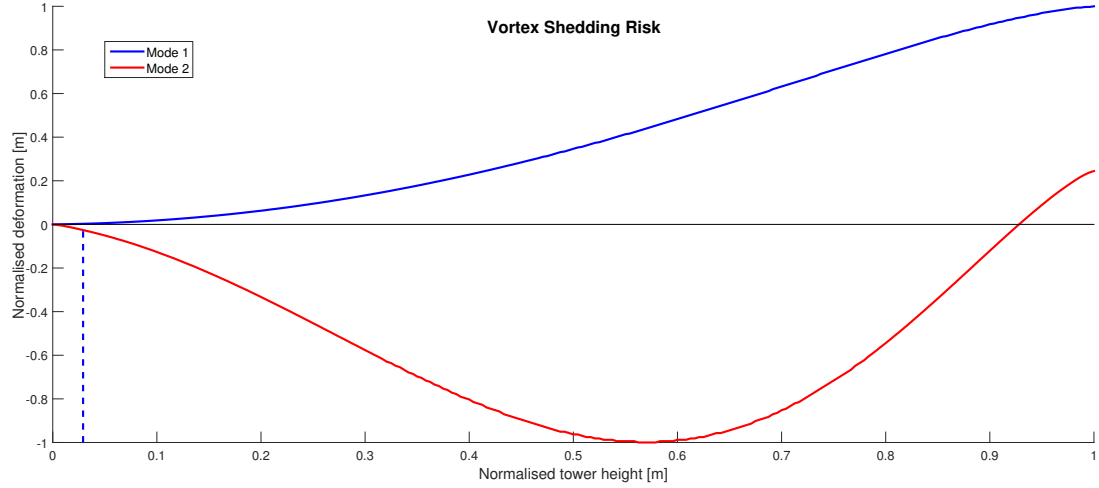


Figure 20: Possible critical vortex shedding induced vibration.

8 Results

This section provides the results from both the analytic and FE-model and conclusions are further discussed in Section 9.

8.1 Analytical Results

External wind pressure

A developed MATLAB function `windpressure.m` calculates the external wind pressure, according to the presented theory in Section 4.1. The external pressure coefficient, which is included in the code, is calculated separately in a function `cpcurve.m`. Implementation of the considered tower height of 120 m results in the graph shown in Figure 21. As can be seen, the pressure is increasing with increasing height, where the minimum value of 200 N/m^2 occurs at the ground level and the maximum value at the top is 910 N/m^2 .

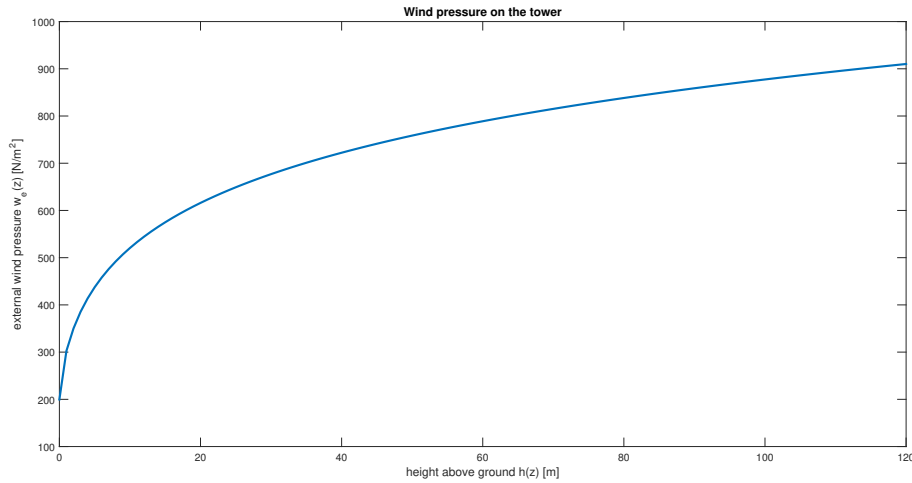


Figure 21: External wind pressure.

Dimensions of the tower structure

Due to adjustments in the model in the end of the thesis project, the preceding results were changed. When the baseline dimensions first was set in the code, the dimensioning curves showed that both of the two materials LVL and GLT clearly exceed the limits of the requirement in both compression and tension. Consequently the baseline dimensions were changed in order to be sufficient to withstand the loading. Calculations with the developed MATLAB code was carried out in order to find a favourable combination of the base diameter and the number of layers in the walls. It turned out that a possible alternative is to have a base diameter of 12.5 m together with five layers at the outside and three layers at the inside. These are the dimensions which are further analysed throughout the project. For the particular examined case, the dimensions are set in the models, in order to verify the developed analytical design tool. In the following a presentation of the baseline dimensions and the examined case study dimensions are performed. Also dimensioning curves for varying shell thicknesses and diameters are shown, in order to observe the behaviour of how the dimensions are affecting the stress in the tower.

Baseline dimensions

Proposed baseline dimensions from Modvion is to have a base diameter of 11.5 m, three LVL layers on the outside and two on the inside, i.e. a thickness of 72 mm and 48 mm respectively. These dimensions are set in the code together with other cross section data and material parameters. The LRFD coefficients presented in Section 3.1 are applied. The design values for load bearing capacity are calculated and compared with design value for resistance in Figure 22.

In the following the design values for the load bearing capacity in tension and compression are denoted as σ_{td} and σ_{cd} for LVL and GLT respectively. Tension strength is illustrated with blue for LVL and red for GLT. Compression strength is illustrated with green for LVL and pink for GLT. The design values for resistance are denoted f_d for each material and marked with dashed lines with matching colours.

In Figure 22 it can be seen that the limit of the requirement in compression for the GLT components are exceeded.

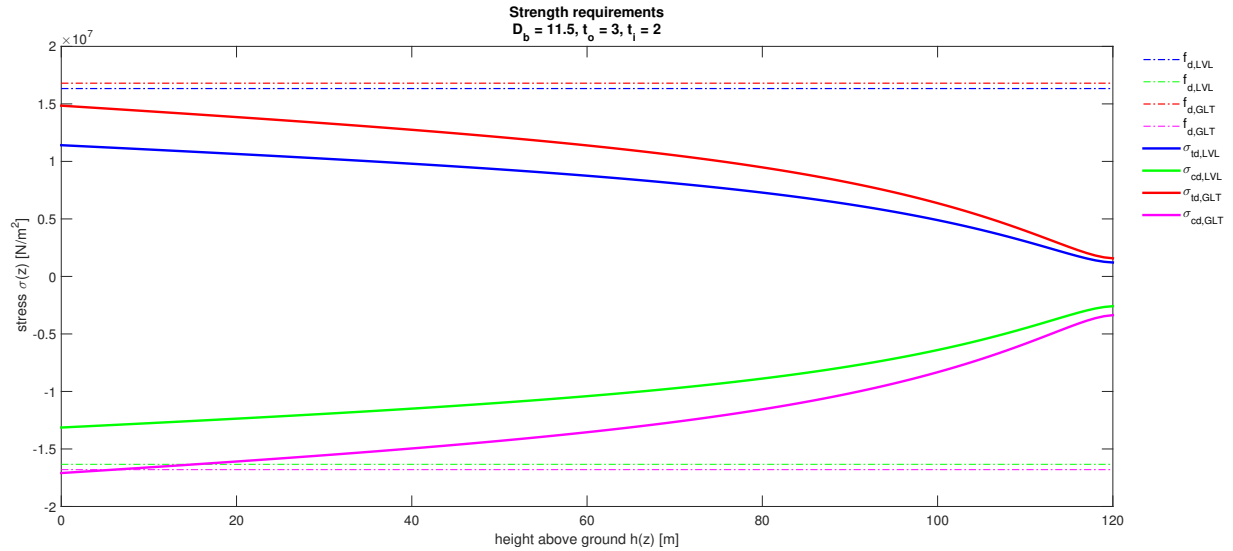


Figure 22: Strength capacity baseline design.

Examined case study

The strength requirements for the analysed dimensions (base diameter 12.5 m, five layers in the outer shell and three at the inner) are shown in Figure 23. For the examined case it can be seen that there is a margin to the allowed strength limit.

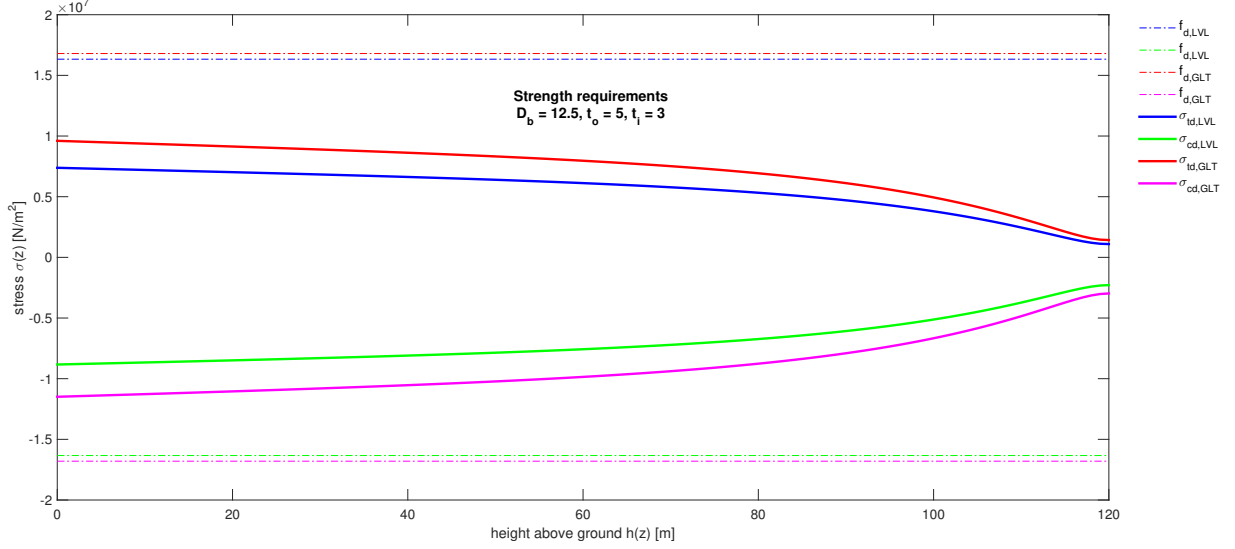


Figure 23: Strength capacity of the tower structure for final obtained dimensions.

Figure 24 presents the bending moment distribution along the tower, where each contribution from the individual load sources are shown. The turbine torque, M_T , constitute the moment M_x around the x-axis and is constant 4.4 MNm along the tower, illustrated by the yellow line. It is considerably lower than the moments acting around the y-axis, i.e. the resulting moment from the wind load M_w and the thrust M_{th} , represented by the dashed red and blue lines respectively. Together these two moments constitute the total moment M_y , illustrated by the purple line in Figure 24. It is as largest at the base, with a value of 156 MNm.

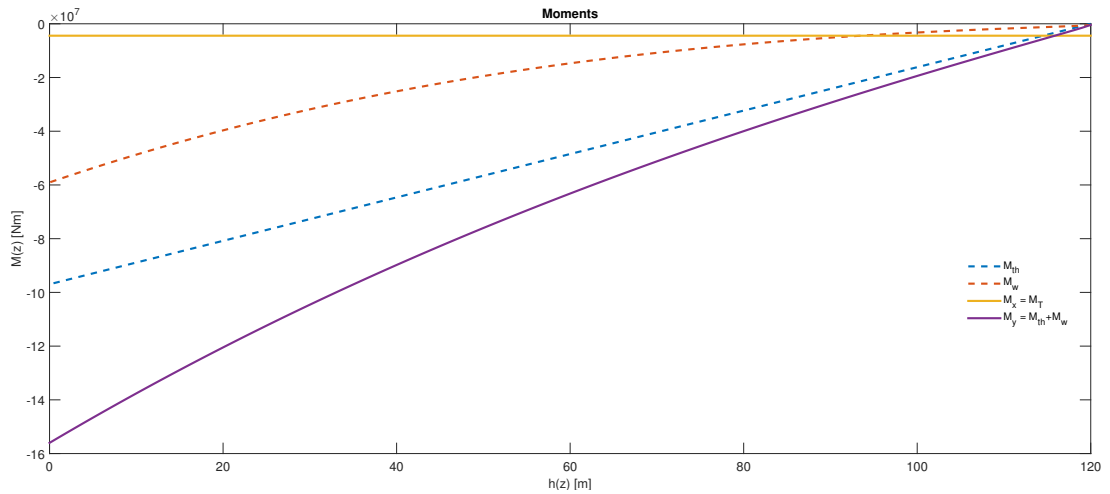


Figure 24: Operating moments obtained from the design loads.

Prescribed moments are recalculated into stress components, illustrated in Figure 25, together with additional stress contributions from the dead weight loading. Clarification of the notations in the graph is summarised below.

Shell axial stress arrived from

σ_w	wind
σ_{th}	thrust
σ_{M_T}	torque
σ_{tow}	self weight tower
σ_{head}	tower head top mass

σ_N	$:= \sigma_{tow} + \sigma_{head}$
σ_{Mx}	$:= \sigma_{M_T}$
σ_{My}	$:= \sigma_{M_w} + \sigma_{M_{th}}$

As the total moment around the y-axis is larger than the one around the x-axis, it follows that the σ_{My} -component of the stress is significantly larger than the σ_{Mx} -component, according to the directions that the loads are applied in, in the assigned coordinate system. Mainly the structure is affected by the thrust that appears at the rotor, which generate a peak value of the stress of 3.3 MPa. The σ_{My} -component has a peak value of 5 MPa at the base and the σ_{Mx} -component 1 MPa at the top. As shown in the figure the normal stress in the tower gives a smaller contribution to the total stress in the tower.

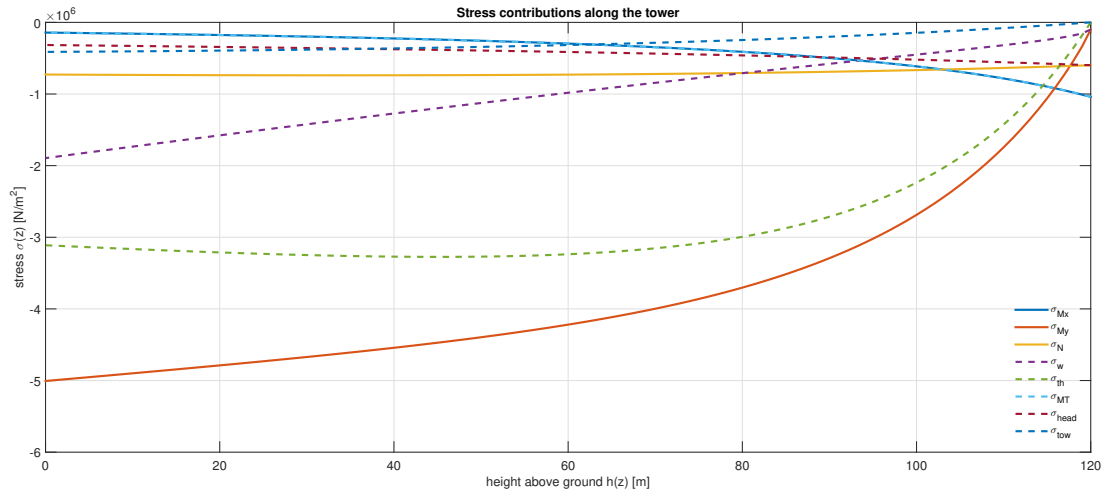


Figure 25: Stress distribution in the tower arrived from the components of the applied design loads.

Combined dimension variables

The following presents the impact of the strength for different tower configurations.

The strength capacity of the tower is showed for a couple of different wall thickness dimensions. The dimensions are measured in terms of number of layers at the outside and inside, denoted NoL_o and NoL_i respectively. The results are reviewed in Figure 28 and Figure 29 for LVL and GLT respectively. It is noted that the GLT beams determines the dimension of the total thickness. The strength criteria can also be observed for varying base diameters shown in Figure 26 and Figure 27.

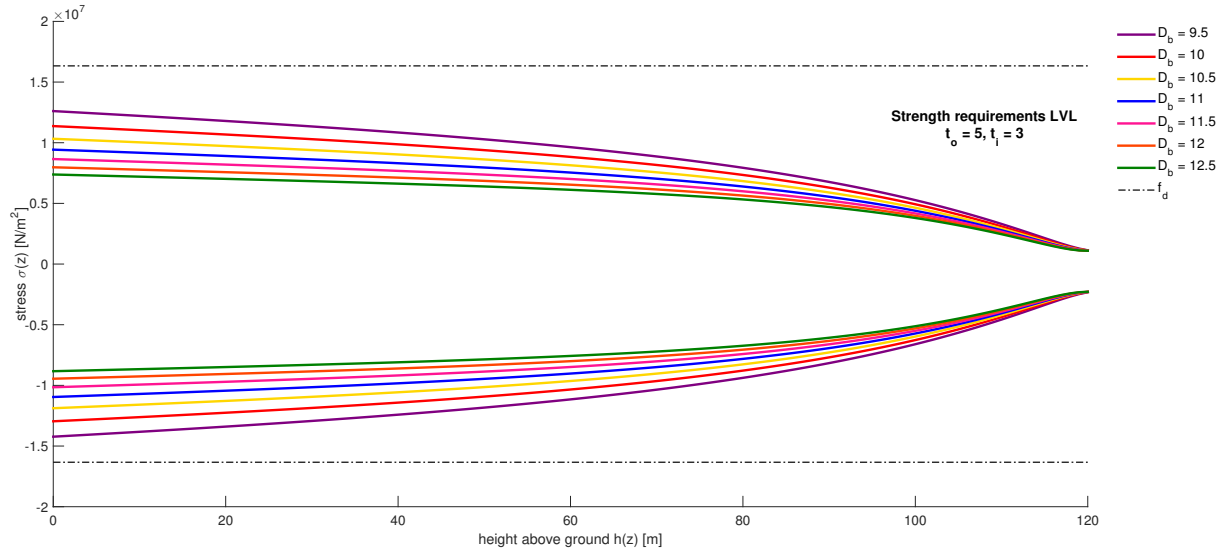


Figure 26: Strength capacity LVL considering different base diameters.

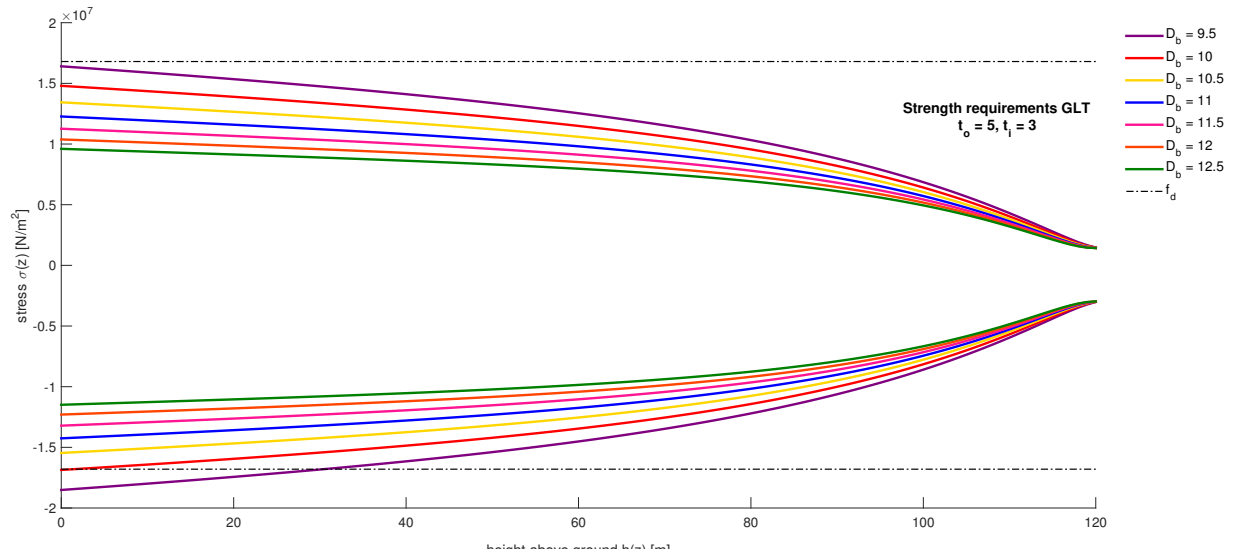


Figure 27: Strength capacity GLT considering different base diameters.

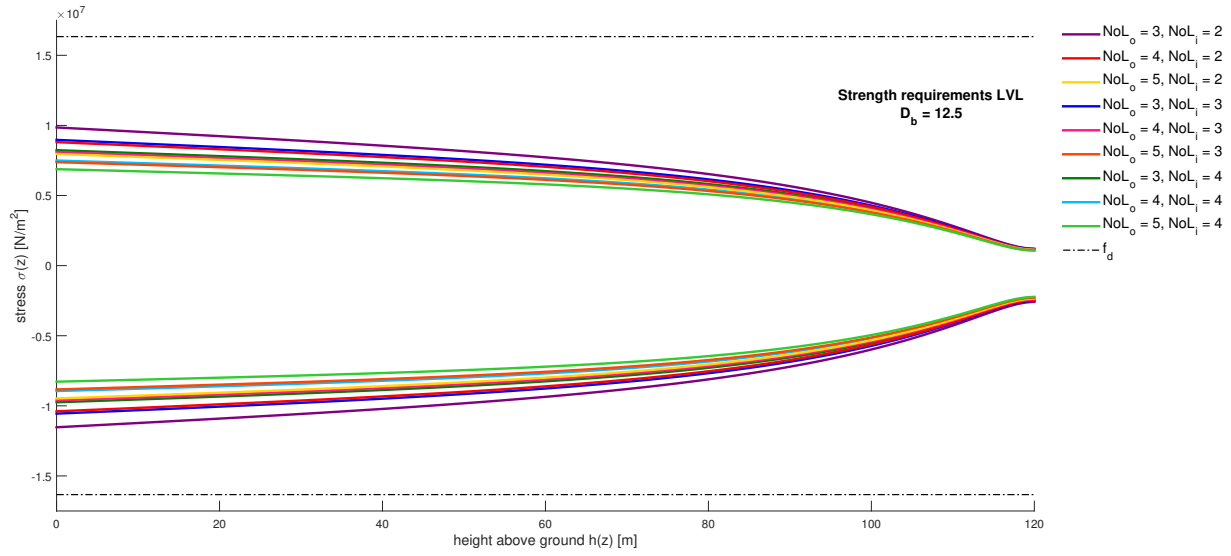


Figure 28: Strength capacity LVL considering a base diameter of 12.5 m and combinations of different shell thicknesses.

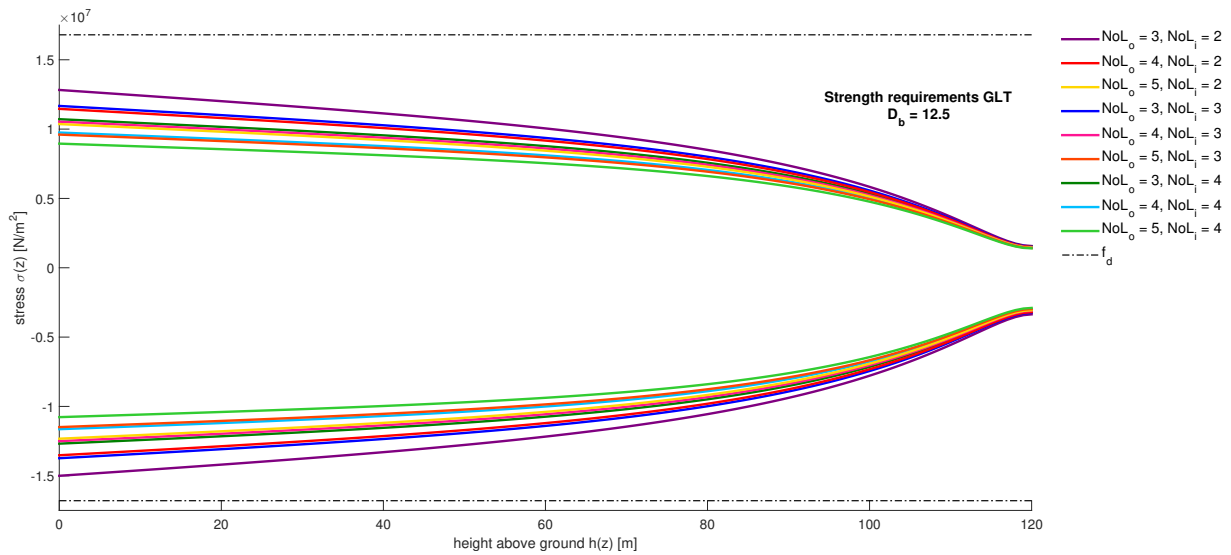


Figure 29: Strength capacity GLT considering a base diameter of 12.5 m and combinations of different shell thicknesses.

Deflection of the tower

The deflection of the tower is calculated using beam theory, according to Section 5.3 with SLS stiffness values.

Figure 30 shows the deflection of the structure calculated for a wall thickness with five and three number of layers in the outer and inner section respectively. The deflection is plotted for a base diameter varying from 9.5 m to 12.5 m and the result of the tower top deflection is presented in Table 7. For a tower base diameter of 12.5 m, the deflection is 0.67 m which is 0.56 % of the total height of the tower.

During operation deformation of rotor blades naturally occurs due to aerodynamic and gravitational forces. A concern is to make sure to keep a distance between the blade tip and the tower, especially under bad weather and wind circumstances when it could be a risk for them to collide. An explicit number of a sufficient distance will have to be included in future work, since geometrical and stiffness parameters of the blades and rotor are specified differently for each turbine. In this work, the NREL reference turbine has been used mainly in order to verify the loads of the tower. As a notice, wind turbines are normally based with an overhang shifted from the tower [6]. Further provisions are commonly made, the rotor axis is often tilted and the blades are coned in order to avoid collision. Overhang, shaft tilt and pre coning for the considered reference turbine is 5m, 5° and 2.5° respectively.

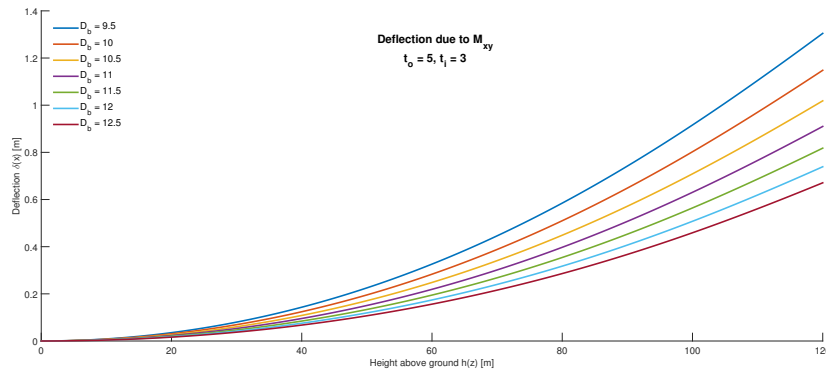


Figure 30: Tower top deflection for different base diameters.

Table 7: Tower top deflection for different base diameters.

Base diameter	Deflection	Percentage of tower height
[m]	[m]	[%]
9.5	1.30	1.09
10.0	1.15	0.96
10.5	1.02	0.85
11.0	0.91	0.76
11.5	0.82	0.68
12.0	0.74	0.62
12.5	0.67	0.56

Tower sectional mass

The tower will be divided in eight sections, each section constituted of four modules that will be assembled at the site. All sections are fifteen meters high and the weight of each part will decrease with height location since the diameter is smaller at the top. It is of interest to know the mass of each section since it will determine the provisions of the machine requirements. Table 8 presents the total weight of each section. Total weight of the tower, including outer and inner panel sections and supporting beams, is 457 tonnes.

Table 8: Mass distribution of tower sections

Height	Mass of
above ground	each section
[m]	[tonnes]
0-15	74.2
15-30	69.3
30-45	64.4
45-60	59.5
60-75	54.6
75-90	49.7
90-105	44.8
105-120	39.9
	Total: 457

8.2 FEM Results

The stress values in the FE-model are compared with the analytical results at the outer most point of the outer shell, summarised in Table 9.

Applying all loads presented in Section 6 resulted in the stress distribution shown in Figure 31 and Figure 32 measured in the axial direction of the tower to be compared with the analytical beam model. The largest tension is located in the lower part on the side where the oncoming wind attain the tower, visualised as the red area in the figure. At the opposite leeward side, the largest compression occurs, visualised in blue colour. The tension and compression stress are 4.2 MPa and 4.5 MPa respectively. Corresponding stress values from the analytical model are 4.3 MPa and 5.7 MPa. The values are below the characteristic allowable stress values for the two materials. More specifically the characteristic tension strength is 19 MPa and 29.5 MPa for LVL and GLT respectively. Subsequently the characteristic compression strength is 19 MPa and 24.5 MPa. This indicates that the dimensions are sufficient to withstand the design loads.

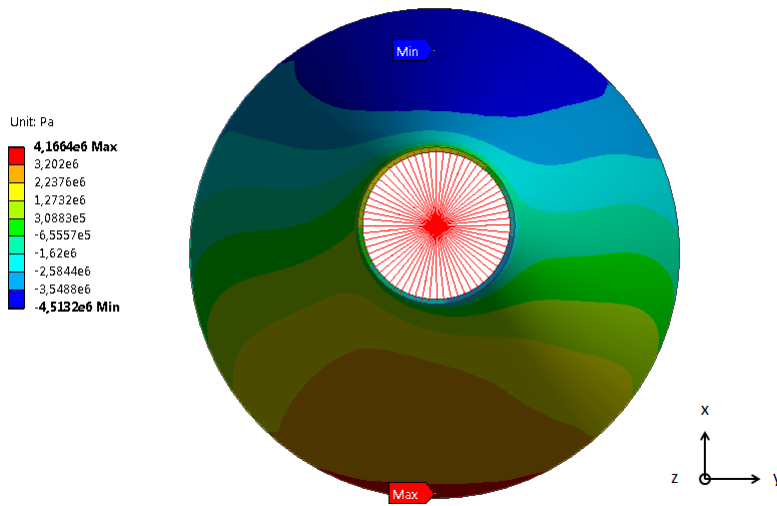


Figure 31: Resulting axial stress levels in the outer shell of the tower, top view.

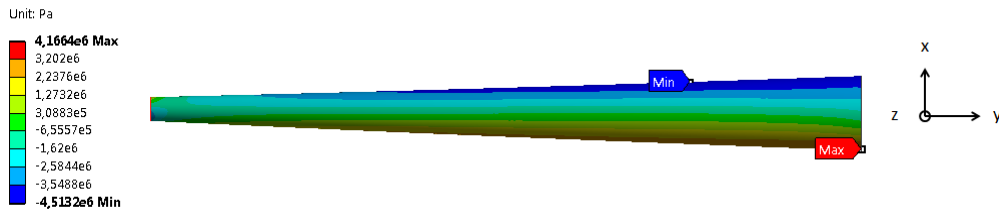


Figure 32: Resulting axial stress levels in the outer shell of the tower, side view.

The two approaches show good resemblance as the stress levels are similar in the FE-model and the analytical model. Small differences are assumed to occur due to the modelling differences according to Section 6; a beam model versus a shell model. The volume of the tower is slightly larger in the FE-model, compare 901 m^3 to 895 m^3 . In addition some of the deviation can probably also be explained by some local bending in the FE-model, which naturally is not present in an analytical model. A difference between the two models appear in the material definition. In the FE-model the two materials are defined as orthotropic and in the analytical beam model only the axial behaviour is considered.

A notation is made regarding the applied wind load, since they are not the same in the two models. Including the end-effect factor $C_{p,e}$ varying in the radial direction resulted in a more realistic distribution of the pressure applied at the outer shell.

Table 9: Comparable stress values from the FE-model and the analytical model

	FE-model [MPa]	Analytical model [MPa]
Gravitational loading		
self weight	0.43	0.41
self weight + top mass	0.76	0.74
Rotor loading		
thrust	3.18	3.27
torque	1.2	1.0
Wind load	1.7	1.9
Total		
Tension	4.17	4.28
Compression	4.51	5.74

Deformation

The deformations of the structure are calculated with the SLS material values. Figure 33 shows the total deformation of the tower, considered in all three directions x-, y-, and z. At the top it has a deformation of 0.59 m which is 0.5 % of the tower height of 120 m, which can be considered as small. The beam model is to regard as conservative compared to the FE-model, since the lateral tower top deflection was calculated to 0.67 m.

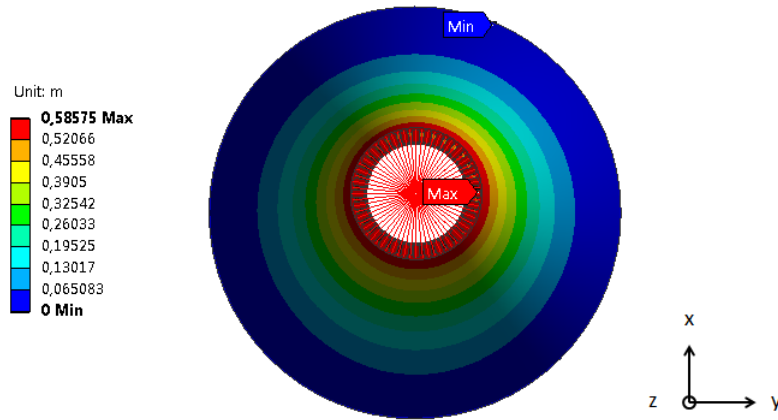


Figure 33: Total deformation.

8.3 Dynamic Results

FAST Simulation²

An analysis of the system is performed in a turbulent and an uniform wind field, described in Section 7.1. Results are presented below.

Turbulent wind field

The wind field generated by TurbSim is shown in Figure 34 and includes three components in x-, y- and z-direction. As can be seen the wind velocity in the x-direction is the dominating one. Firstly, the results from three simulations will be presented which each has different initial conditions of the rotor speed. All simulations are done using the same wind field. Attended initial rotor speeds are 0, 3 and 12.1 rpm. Remember that the cut-in rotor speed and the rated rotor speed is 3 and 12.1 rpm respectively. These rates are chosen in order to observe the turbine response during the start-up transient and normal operation, to be able to identify possible significant behaviour. Nevertheless, the simulations are primarily done to verify the loading of the tower in a time variant system. Thus a more thoroughly presentation of the result from the simulation with an initial rotor speed of 12.1 rpm is presented later on.

Figure 35 shows how the rotor speed is varying over time for the three cases. It is noted that it takes relatively long time until the start-up transient is passed. It is considered to be stabilised, i.e. reached the rated rotor speed, after approximately 20 and 60 seconds for an initial rotor speed of 0 and 3 rpm respectively. Figure 36 shows a similar response, where it can be seen that it takes time until the generator starts to load and generate electrical power output. These responses are assumed to occur since at the beginning of the simulation the turbine is in equilibrium and instantly subjected to the wind load, thus the first part of the simulation can be ignored, considering the reaction forces and moments as well as the displacement in the tower top.

For the cases where the initial rotor speed is 0 and 3 rpm it naturally appears that the yaw bearing force in x- and y-direction, as well as the rotor torque is increasing subsequently as the rotor speed is increasing. More specifically, an increase in the amplitudes of the reaction forces/moment are developed in line with the steep increase of the rotor speed. Potential problems with excited frequencies are discussed further down.

²Late in the process of the thesis work a correction of the calculations were pursued, which affected the tower eigenfrequencies. All calculations and results carried out with the FAST tools are therefor reported with the old values. The first and second tower eigenfrequency changed from 0.29197 Hz and 1.1544 Hz to 0.29849 Hz and 1.731 Hz respectively. The updated adjustments resulted in a stiffer tower structure which increased the frequencies slightly.

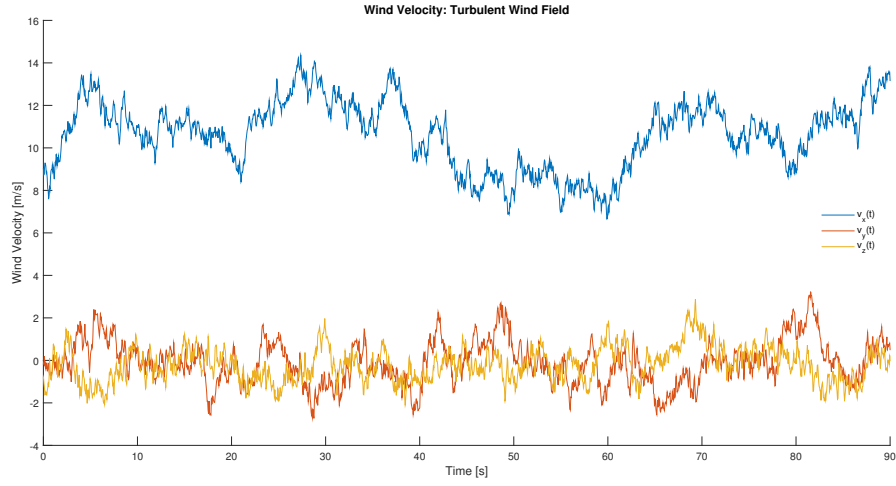


Figure 34: Wind Velocity components.

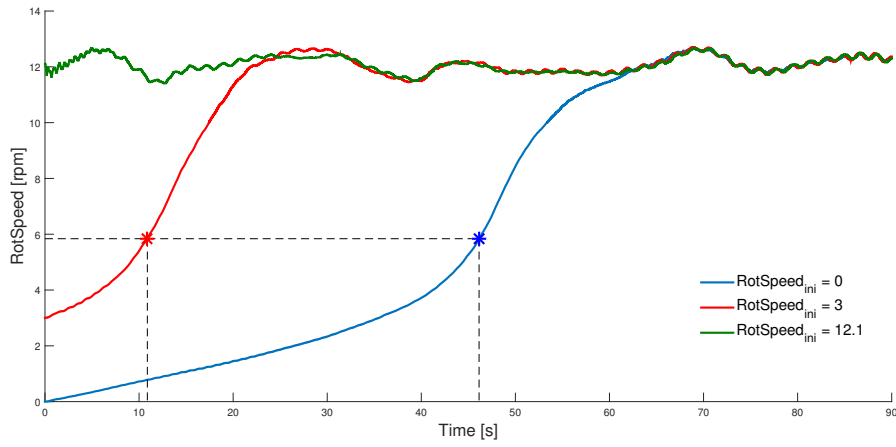


Figure 35: Rotor Speed for initial rotor speed of 0, 3 and 12.1 rpm.

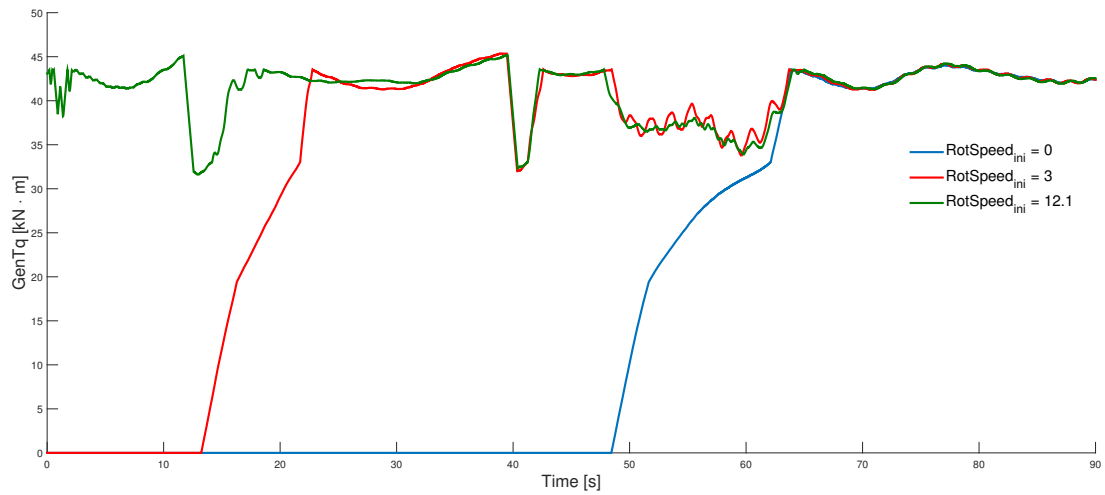


Figure 36: Generator torque for initial rotor speed of 0, 3 and 12.1 rpm.

In order to compare the analytically calculated rotor torque and thrust in operating condition, a longer simulation with a (rated) rotor speed of 12.1 rpm is performed in the turbulent wind field. The simulation has a duration time of 180 seconds, but the results are extracted from ten seconds and forward, due to the imbalance of the turbine in the initial phase. The results are presented in Table 10, together with the results from the analytical calculations and the uniform wind field simulation. Figure 37 shows how the rotor speed is varying over time correspondingly with the wind velocity variation. It is noted that an increase in the wind velocity creates a quick response in the rotor speed.

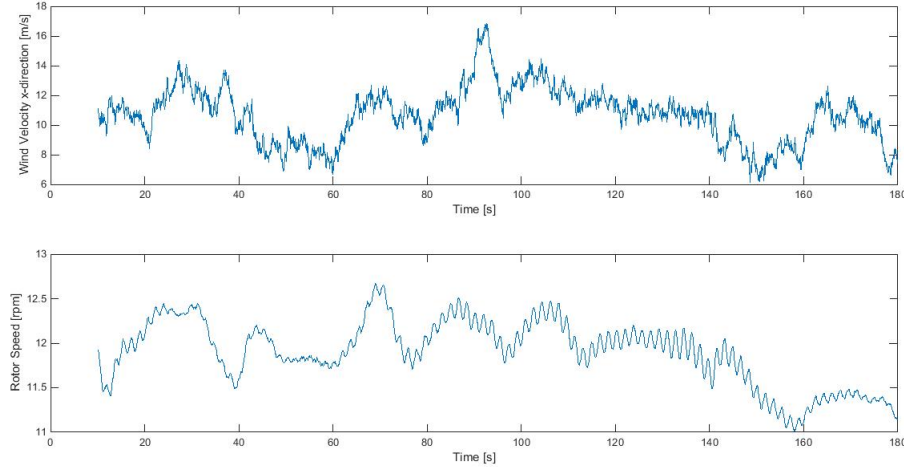


Figure 37: Wind velocity and rotor speed during simulation in a turbulent wind field with initial rotor speed of 12.1 rpm.

The fluctuation of the yaw bearing force at the top of the tower is illustrated in Figure 38, where it is divided into components in x-, y- and z-direction. Comparable thrust calculated in the analytical model is a resultant of the x- and y-component, thus these are shown separately in Figure 39. It can be seen that the contribution in the y-direction is considerable smaller and that the main part is originated in the x-direction, which is the direction of the wind flow. It is also noted that the yaw bearing force in z-direction is 3.48 MN, which can be considered to correspond to the gravitational loading from the nacelle head (tower top mass defined as 349 tonnes in the FAST model).

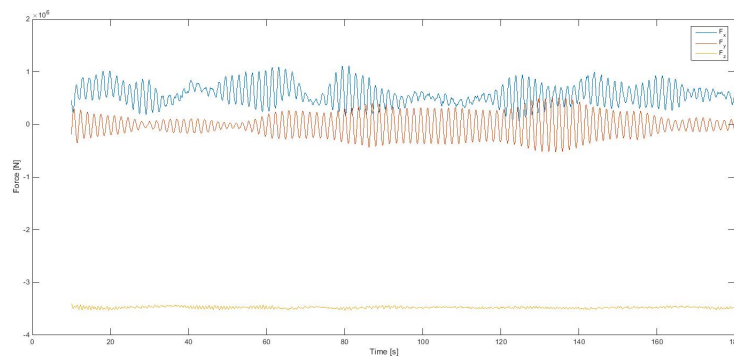


Figure 38: Force reaction in x- y- and z-direction during simulation in a turbulent wind field with an initial rotor speed of 12.1 rpm.

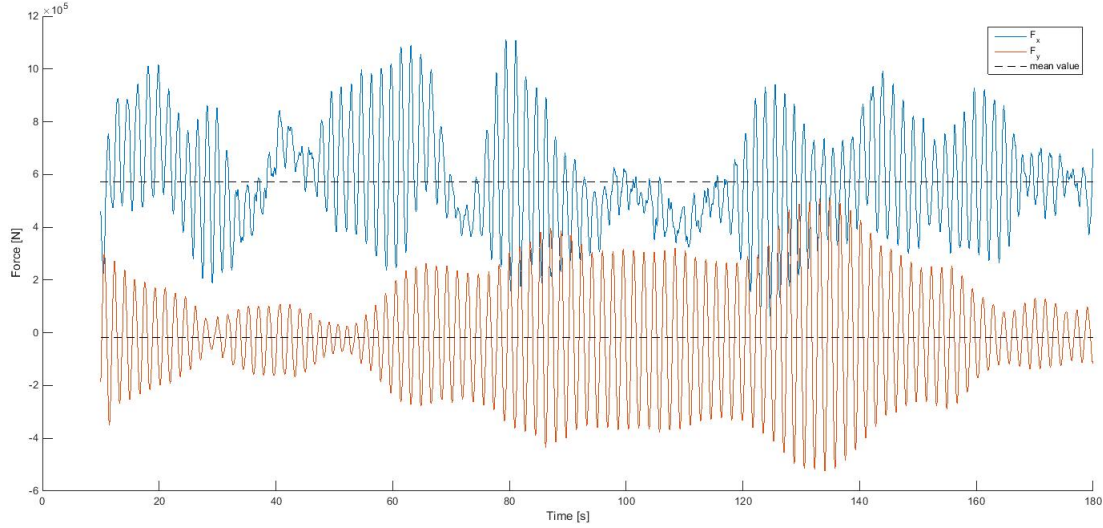


Figure 39: Force reaction in x- and y-direction during simulation in a turbulent wind field with an initial rotor speed of 12.1 rpm.

Mean and maximum values of all three force components are presented in Table 10. The resultant thrust force, composed of the x- and y-component is shown in Figure 40 where the mean value of 0.61 MN is marked with a striped black line. To compare with the static analytically calculated thrust with a value of 0.81 MN it is 25 % difference. The large difference can be explained by the difference in both the magnitude of the rotor speed and wind velocity. The analytically calculated rotor thrust is determined by a mean wind velocity over the rotor at 11.5 m/s inflowing wind and a rotor speed of 12 rpm. In the turbulent wind simulation, the wind velocity is below 11.5 m/s during 68 % of the time and below 12 rpm during 56 % of the time. Accordingly, the dynamic simulation provides a smaller mean value of the thrust. As follows it can be said that the analytical calculation is conservative, representing a "worst case scenario" and it is not constantly subjected to this large load. However, due to the natural variation of the wind velocity (and other phenomena such as turbulence, gust etc) it is occasionally subjected to larger loads. As an example, the maximum value during the observed time frame is 1.15 MN. The force peaks fluctuating around the mean value are considered to not influence markedly in the studied case, since the period is regarded to short to have an influence of the deflection of the tower.

Furthermore, the resultant thrust is converted to a smoother signal in order to better see the relation with the rotor speed varying over time, hence easier to identify possible excitation frequencies discussed further down. This is presented in Figure 41 where it clearly can be seen that both the thrust and the rotor speed are fluctuating in a similar way, influenced by the wind velocity variation.

Figure 42 shows how the rotor torque is fluctuating over time. Naturally, the maximal torque of 4.7 MNm appears at the same time as the maximum thrust force. A mean value of the torque is conservatively extracted in the time frame between 64 and 140 seconds, since this period represents the largest load. The mean value during this period is 4.2 MNm, to compare with the static analytically calculated torque of 4.4 MNm, it is a difference of 6 %.

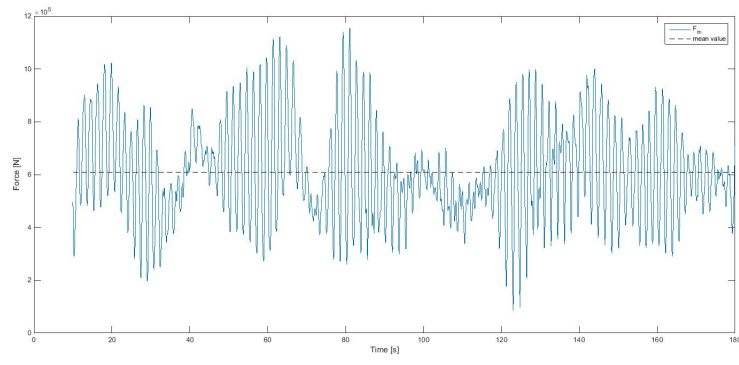


Figure 40: Thrust.

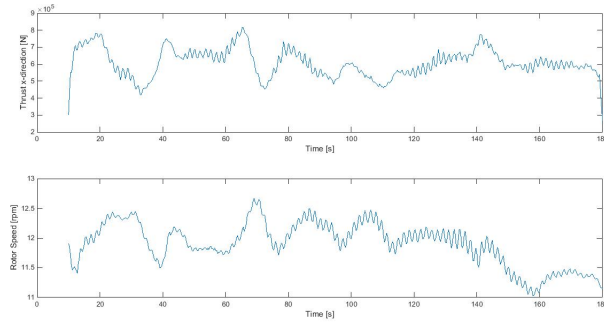


Figure 41: Thrust (smoothed signal) and rotor speed.

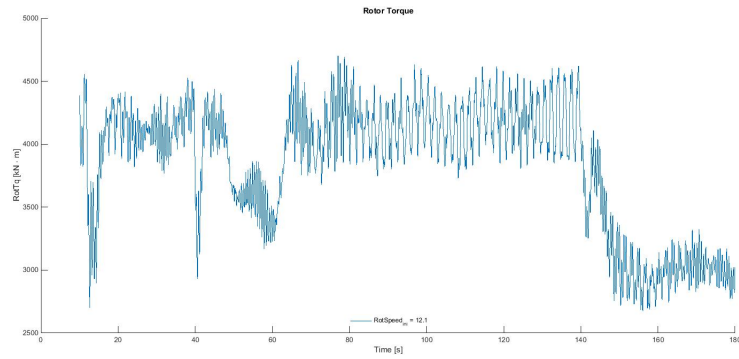


Figure 42: Rotor torque during simulation in a turbulent wind field with an initial rotor speed of 12.1 rpm.

Figure 43 and 44 shows the tower top displacement in fore-aft and side-to-side respectively, measured from the centre line of the tower, versus the force at the same location. They are plotted in such a way that the mean values of the force and the displacement coincide, marked with a black line in each figure. It can clearly be seen that the force and displacement variation act in accordance with one another. At the time that a force increment or decrements appears, correlating displacement develops. The deflection of the tower is largest in fore-aft direction, since the force component also is largest in this (wind) direction. The mean deflection in fore-aft is 0.11 m and side-to-side -0.03 m. Together they add up to a displacement of 0.11 m. This is to be considered as small in the context, due to the large dimensions of the tower. The mean displacement at the top is only 0.1 % of the total tower height. During the time that the force is as largest, a maximum displacement of 0.24 m is surveyed in the simulation, which also is small since it is 0.2 % of the tower height.

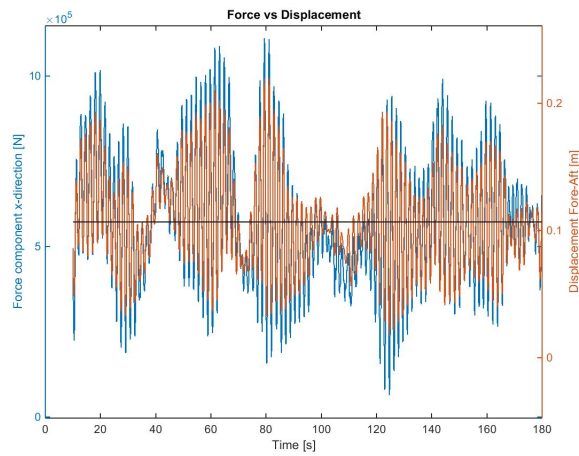


Figure 43: Force and displacement in x-direction, obtained from the turbulent wind field simulation.

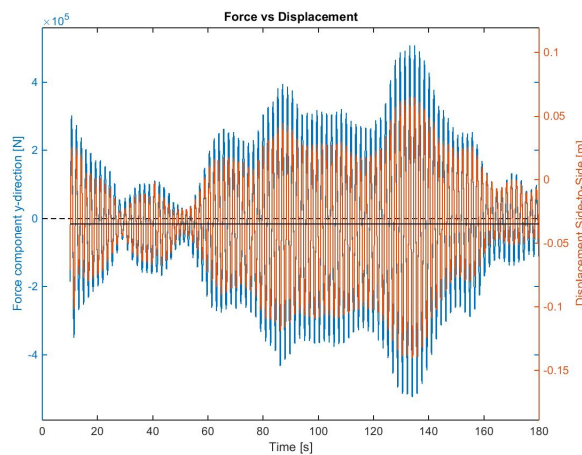


Figure 44: Force and displacement in y-direction, obtained from the turbulent wind field simulation.

Table 10: Comparison of loads and deflection

Parameter	Turbulent Wind Field		Uniform Wind Field		Analytical
	Rotor Speed: 12.1 rpm		Rotor Speed: 12 rpm		
	Simulation time: 10-180 seconds		Simulation time: 10-180 seconds		
Wind Vel.	Unit	Mean	Max	Mean	Max
	[m/s]	10.7	16.8	12	12
Rot. Speed	[rpm]	11.9	12.7	12	12
M_T	[MNm]	4.2	4.7	4.2	4.4
F_x	[MN]	0.57	1.11	0.73	0.79
F_y	[MN]	-0.02	0.52	-0.01	0.21
F_z	[MN]	-3.48	3.53	-3.49	-3.46
F_{th}	[MN]	0.61	1.15	0.73	0.82
δ_{FA}	[m]	0.11	0.22	0.13	0.14
δ_{SS}	[m]	-0.04	0.14	-0.04	0.08
δ_{tot}	[m]	0.12	0.24	0.14	0.16
					0.67

Uniform wind field

A simulation in a uniform wind field is performed in order to compare the magnitude with the analytical calculations of the rotor torque and thrust. Both of these loads, stated in Equation 18 and 16, are calculated with an average wind speed of 11.5 m/s over the rotor in the analytical model, thus this value is used in the dynamic simulation. Furthermore, since the torque (Equation 18) is calculated for a rotor speed of 12 rpm it is the considered value in the analysis. Figure 45 to 47 shows the results for this set up, including the tower configuration. The results are plotted from 30 seconds, since the first time frame is not of interest for the reason that it takes some time until the calculation model is stabilised.

Figure 45 illustrates how the mechanical rotor torque at the top of the tower is varying over time. The mean value is 4.20 MNm and the maximum value is 4.43 MNm. Compared with the analytical calculation, it is a difference of 5.5 % and 1.5 % respectively. The yaw bearing force at the top is divided into three components in x-, y- and z-direction. Since the thrust is a resultant of the force components in x- and y-direction, they are plotted separately in Figure 46. As in the turbulent simulation, the force component at the tower top in the x-direction is the dominating one having a mean value of 0.73 MN. The mean value in y-direction is -0.0096 MN which gives the mean resultant rotor thrust 0.73 MN. It is 9.3 % difference from the analytical calculation. The maximum value noted in the simulation time frame (10-90 seconds), in x- and y-direction respectively, is 0.79 MN and 0.21 MN. It results in a maximum thrust of 0.82 MN. The force in z-direction, which has a mean value of 3.49 MN, is as mentioned before considered to represent the gravitational loading of the tower head mass (349 tonnes in the simulation).

Figure 47 shows the displacement of the tower top, measured from the centre line of the tower. It can clearly be seen that the tower is slightly displaced from the centre line and oscillating symmetrically back and forth around the mean values marked with the dashed black lines. The mean translational deflection in fore-aft and side-to-side is 0.13 m and 0.04 m respectively, which adds up to a resultant 0.14 m. Considering the maximum deflection of 0.14 and 0.08 m in fore-aft and side-to-side, this means that the tower is shifted 0.01 m and 0.04 m from the "new" state of equilibrium. The maximum resultant displacement is 0.03m, which means that the tower in total is oscillating 0.16 m from the "new" equilibrium position.

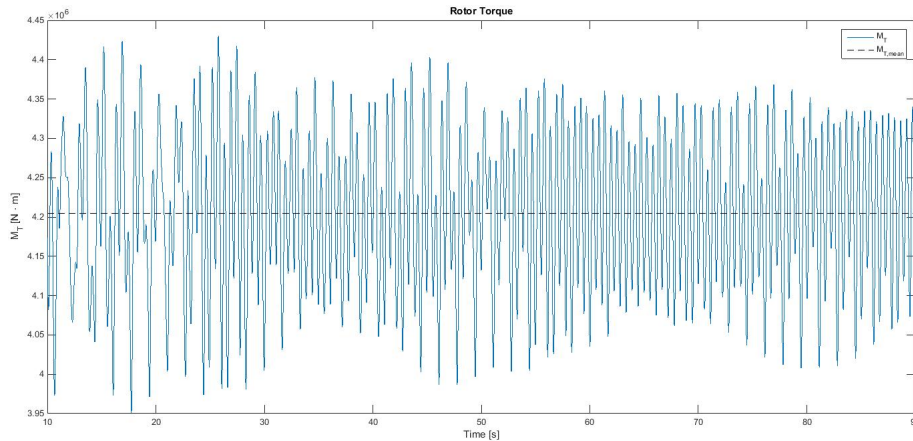


Figure 45: Rotor torque during simulation in a uniform wind field.

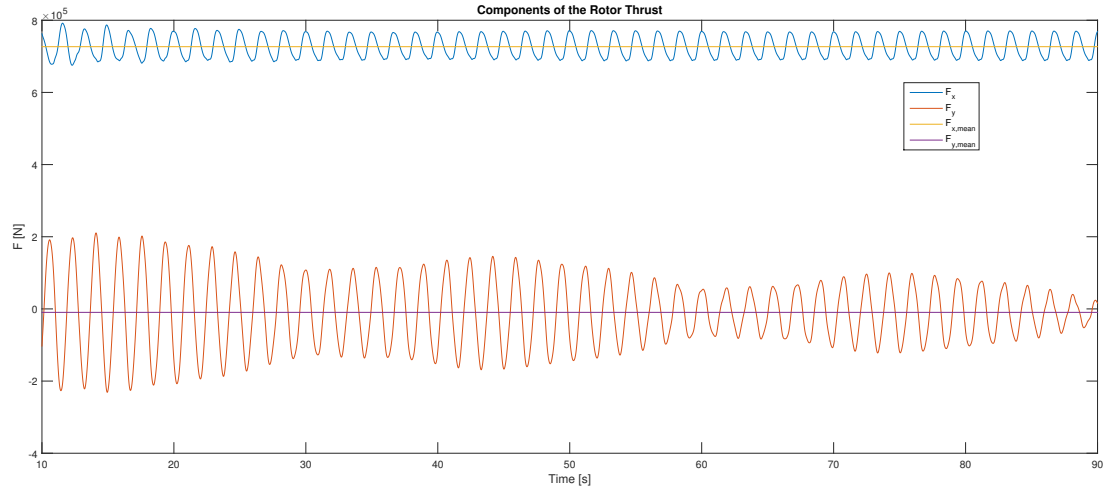


Figure 46: Force components at the tower top during simulation in a uniform wind field.

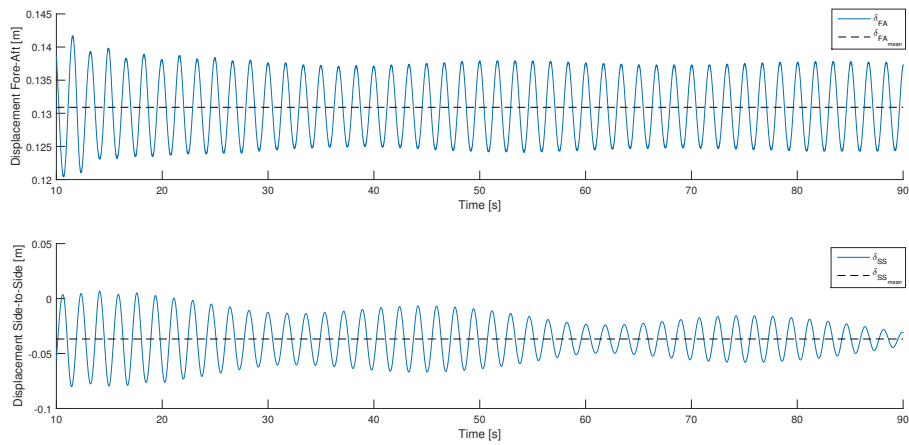


Figure 47: Displacement at the tower top during simulation in a uniform wind field.

Excitation Problems

The first bending frequency of the tower was confirmed to lie within 1P and 3P, which is of importance to not cause excitational loading during operation. However, during a start up the natural tower frequency will coincide with the rotor frequency for a shorter time and it is of importance that this phase is passed quickly. It was noted in Figure 35 that the frequency corresponding to 5.8 rpm was passed during the start up transient. Since this stage is passed considerably fast it showed no specifically notable sign of being a problem, only a small increase in force and corresponding displacement for a short period.

It was observed in Section 7.2 that vortex shedding induced loads might occur around 4 m height. As also was mentioned this is not considered as an issue due to the form of the first mode shapes. It is illustrated in Figure 20 Section 7.2, where it can be seen that the percental displacement at this points is likely too small to cause any oscillation.

The excitation load is something that is gradually developed, caused by the process where increasing deformation leads to larger loads and vise versa until it is oscillating with undesirable amplitude. The tower structure is very stiff, hence it is probably not likely that exaggerated vibrations would be developed. Nor at the above stated point or during the short transient period during a start up of the rotor. Deformations shown in the analysis are too small. However, the transient period should be further studied in the future when a specific turbine is decided to operate at the tower structure.

9 Discussion and Conclusion

In this study the conceptual design of a wooden wind power tower is analysed. A computational tool is established in order to examine the dimensions of the cross sectional components. The acceptable layout of the cross section is determined by comparing the total load and resistance curves of each configuration, shown in Section 8.1. When applying the load factors, the compression and tension in the outer shell increased to 8.8 MPa and 7.4 MPa. This was compared with the resistance value of $f_{m,d} = 15.68$ MPa for LVL. It was also checked that the GLT elements passed the strength requirements for the determined dimensions. The actual characteristic bending strength f_m for LVL, which is the dominating material in the structure, is 28 MPa. If this value should be compared with the actual stress in the tower of 5.7 MPa in compression and 4.3 MPa in tension, one can see that the determined number of layers in the shells are regarded sufficient.

A notation is also made regarding the partial coefficients and safety factors that were applied according to Eurocode. The design codes are stipulated for all kinds of buildings in order to have safety margin in architectures where people are present. The margins of safety is not appropriate for wind turbine towers, since people are generally not allowed to occupy the area around these structures. For that purpose the margins are regarded too conservative when applied to a wind tower structure, which exaggerates the dimensions.

It can be concluded that the developed analytical approach is a useful tool for an initial structural design of the tower. It was verified that the basic results from the analytical and FE-model correspond well. Dimensions of the cross sectional elements of the tower that are examined in this thesis project are sufficient for the applied global design loads. In the context it should also be mentioned again that the materials are modelled as orthotropic in the FE-model which also makes a difference in the results. In a succeeding project work the next step can be to observe the LVL plates in more detail, structured individual number of layers instead of a homogeneous cross section.

Due to the final adjustments in the models, it turned out that the cross sectional dimensions possibly can be reduced. Although the tower with reduced dimensions is capable to withstand the loads, it might not necessarily be a better alternative. A smaller base diameter could cause excitation frequency problems and/or cause too large deformations of the structure. An investigation with a future actual turbine would be necessary, as well as a computational fluid dynamics analysis or wind tunnel experiment. The tower top deflection is also to regard as a dimensioning factor. With reduced dimensions the deformation will increase. It will be of interest to know the allowed deflection, which is dependent on the choice of turbine, also discussed in the section of the analytical results.

The results from the dynamic model (Section 8.3) implemented with the FAST tools showed that the analytically determined loads were conservatively estimated. Comparable thrust was 25 % and 9 % smaller in the turbulent and uniform wind field respectively. The analytically calculated torque is closer to results from the dynamic analysis, which showed a 6 % difference in the turbulent and uniform condition. Thus, the simulation in the uniform wind field yields a more similar result to the analytical calculation than the turbulent wind field simulation.

Regarding the deflections it can be noted that the obtained tower top displacement in the dynamic model appear to be remarkably low, and would probably be lower if the correct

input data was implemented since these resulted in a stiffer structure. A possible reason for the lateral deflection differences in the models is that the dynamic varying load results in smaller deformation than a quasistatic load which is acting constantly. It is declared that the input data to the FAST simulations were made with the old tower properties, i.e. before the calculations were modified and that the results should be carefully observed. The dynamic simulations were primarily carried out to verify and compare the quasistatic loads implemented in the analytical calculations. Since the fictive turbine that was observed in this project do not exists in reality, an analysis with a future specific turbine must be carried out in order to observe the response.

To sum up the results implies that the examined dimensions of the tower geometry most likely are on the safe side applying the design loads and given circumstances of a future location of the tower. Though there are several more conditional scenarios that has to be tested and analysed in more detail. Among the cases, emergency shut down, sudden loss of wind and extreme storm weather etc., also a more thoroughly analysis of start up and shut down transients in different weather conditions. In a future actual case it is important to implement the right coefficients in the wind load calculations, found in the formulas stated in Eurocode, which is based on the location of the tower, as well as implementing a certain turbine.

For future reference the design has to be studied in more detail considering bonding of the modules, base foundation, nacelle attachment etc. Applicable bonding of the panels are of great importance in order to endure all operating cases. Furthermore it will be of interest to investigate how much the strength capacity will increase when implementing additional not showed stiffening elements in the design. An essential study will also be to analyse long term effects such as fatigue in the structure, due to the constantly subjection of dynamic loading by wind and rotor.

References

- [1] Jonkman et. al. *Definition of a 5-MW Reference Wind Turbine for Offshore System Development*. Tech. rep. NREL/TP-500-38060. National Renewable Energy Laboratory, a national laboratory of the U.S. Department of Energy, Feb. 2009.
- [2] Ottosen et. al. *Introduktion till hållfasthetslära: enaxliga tillstånd*. Upplaga 1. Studentlitteratur, 2007.
- [3] Eric Borgström. *Design of timber structures - Rules and formulas according to Eurocode 5*. Vol. 2. Swedish Forest Industries Federation, 2016.
- [4] *Boverket mandatory provisions amending the board's mandatory provisions and general recommendations (2011:10) on the application of European design standards (Eurocodes)*, EKS. Tech. rep. Boverket, 2013.
- [5] Svend Ole Hansen. *Vortex-induced vibrations of structures*. Tech. rep. Structural Engineers World Congress 2007.
- [6] Erich Hau. *Wind Turbines*. 2nd Ed. Springer-Verlag Berlin Heidelberg, 2006.
- [7] A.L Rogers J.F Manwell J.G McGowan. *Wind Energy Explained*. 2nd Ed. John Wiley & Sons Ltd., 2009.
- [8] B.J. Jonkman and Jr. M.L. Buhl. *TurbSim User's Guide*. Tech. rep. NREL/TP-500-38060. NREL/TP-500-39797, September 2006.
- [9] *Modvion AB*.
<http://www.modvion.com/>.
- [10] *NWTC Information Portal, Excel file obtained in communication forum, uploaded March 2012 by J. Jonkman*.
<https://wind.nrel.gov/forum/wind/viewtopic.php?t=582>. Accessed 16-October-2017.
- [11] *NWTC Information Portal (FAST). Last modified 19-March-2015*.
<https://nwtc.nrel.gov/FAST>. Accessed 11-October-2017.
- [12] Jack Porteous and Abdy Kermani. *Structural Timber Design to Eurocode 5*. John Wiley & Sons, Incorporated, 2013.
- [13] Bungale S. Taranath. *Structural Analysis and Design of Tall Buildings - Steel and Composite Construction*. 2nd Ed. Taylor & Francis Group, LLC, 2012.
- [14] Directive 2004/18/EC The European Union Per Regulation 305/2011 Directive 98/34/EC. *Eurocode 1: Actions on structures - Part 1-4: General actions - Wind actions. EN 1991-1-4 (2005)*. Tech. rep.
- [15] S. Thelandersson and H. J. Larsen. *Timber Engineering*. John Wiley & Sons Ltd, 2003.
- [16] Svenskt Trä. *Limträhandbok - Fakta om limträ del 1*. Föreningen Sveriges Skogsindustrier, 2016.

Appendix

Appendix A: Dynamic Analysis

A1. Input properties FAST ³

Table 11: Distributed input tower properties

Fractional Height [-]	Mass Density [kg/m]	Stiffness [Nm ²]
0.0	$4.191 \cdot 10^3$	$1.134104 \cdot 10^{12}$
0.1	$4.392942 \cdot 10^3$	$9.478141 \cdot 10^{11}$
0.2	$4.165517 \cdot 10^3$	$7.678135 \cdot 10^{11}$
0.3	$3.938 \cdot 10^3$	$6.121959 \cdot 10^{11}$
0.4	$3.710575 \cdot 10^3$	$4.791852 \cdot 10^{11}$
0.5	$3.483058 \cdot 10^3$	$3.6752 \cdot 10^{11}$
0.6	$3.255633 \cdot 10^3$	$2.738798 \cdot 10^{11}$
0.7	$3.028117 \cdot 10^3$	$1.980327 \cdot 10^{11}$
0.8	$2.8692 \cdot 10^3$	$1.376879 \cdot 10^{11}$
0.9	$2.573175 \cdot 10^3$	$9.106921 \cdot 10^{10}$
1.0	$2.34575 \cdot 10^3$	$5.644 \cdot 10^{10}$

Table 12: Polynomial coefficients

Mode	Frequency [Hz]	Polynomial Coefficient				
		x^6 -term	x^5 -term	x^4 -term	x^3 -term	x^2 -term
FA1	0.29197	0.1847	-0.9244	1.0510	-0.3993	1.0880
FA2	1.1544	-11.1800	23.2000	-17.1900	12.2600	-6.0920
SS1	0.29197	0.2344	-1.0710	1.2110	-0.4759	1.1020
SS2	1.1544	-10.9300	22.6400	-16.7800	12.1400	-6.0850

³Late in the process of the thesis work a correction of the calculations were pursued, which affected the tower eigenfrequencies. All calculations and results carried out with the FAST tools are therefor reported with the old values. The first and second tower eigenfrequency changed from 0.29197 Hz and 1.1544 Hz to 0.29849 Hz and 1.731 Hz respectively. The updated adjustments resulted in a stiffer tower structure which increased the frequencies slightly.

A2. Vortex Frequencies

Table 13: Vortex frequencies f_{vortex} [Hz] at reference height z [m].

z	f_{vortex}	z	f_{vortex}	z	f_{vortex}	z	f_{vortex}
0	-	31	0.5335	62	0.7511	93	1.0887
1	0.2061	32	0.5399	63	0.7594	94	1.1034
2	0.2552	33	0.5462	64	0.7678	95	1.1185
3	0.2849	34	0.5526	65	0.7764	96	1.1340
4	0.3067	35	0.5590	66	0.7851	97	1.1499
5	0.3242	36	0.5654	67	0.7939	98	1.1661
6	0.3390	37	0.5718	68	0.8029	99	1.1827
7	0.3520	38	0.5782	69	0.8120	100	1.1998
8	0.3636	39	0.5847	70	0.8213	101	1.2173
9	0.3743	40	0.5912	71	0.8307	102	1.2352
10	0.3842	41	0.5978	72	0.8403	103	1.2536
11	0.3934	42	0.6044	73	0.8500	104	1.2725
12	0.4022	43	0.6111	74	0.8599	105	1.2919
13	0.4106	44	0.6178	75	0.8700	106	1.3119
14	0.4186	45	0.6245	76	0.8802	107	1.3324
15	0.4264	46	0.6314	77	0.8906	108	1.3535
16	0.4339	47	0.6382	78	0.9013	109	1.3752
17	0.4412	48	0.6452	79	0.9121	110	1.3976
18	0.4483	49	0.6522	80	0.9231	111	1.4206
19	0.4553	50	0.6593	81	0.9344	112	1.4443
20	0.4622	51	0.6664	82	0.9458	113	1.4688
21	0.4690	52	0.6737	83	0.9575	114	1.4940
22	0.4756	53	0.6810	84	0.9694	115	1.5200
23	0.4822	54	0.6884	85	0.9816	116	1.5468
24	0.4888	55	0.6959	86	0.9940	117	1.5746
25	0.4952	56	0.7035	87	1.0067	118	1.6033
26	0.5017	57	0.7112	88	1.0196	119	1.6330
27	0.5081	58	0.7189	89	1.0328	120	1.6637
28	0.5145	59	0.7268	90	1.0463		
29	0.5208	60	0.7348	91	1.0601		
30	0.5272	61	0.7429	92	1.0742		